https://doi.org/10.5194/egusphere-2023-304
Preprint. Discussion started: 28 March 2023

Land-cover and management modulation of ecosystem resistance to drought stress

Chenwei Xiao[1], Sönke Zaehle[2], Hui Yang[1], Jean-Pierre Wigneron[3], Ana Bastos[1]

[1]Department for Biogeochemical Integration, Max Planck Institute for Biogeochemistry, Jena, Germany
[2]Department of Biogeochemical Signals, Max Planck Institute for Biogeochemistry, Jena, Germany
[3]INRAE, UMR1391 ISPA, Université de Bordeaux, F-33140 Villenave d'Ornon, France

Correspondence to: Chenwei Xiao (cxiao@bgc-jena.mpg.de)

Abstract. Drought events are projected to become more severe and frequent across many regions in the future, but their impacts will likely differ among ecosystems depending on their ability to maintain functioning during droughts, i.e., ecosystem resistance. Plant species have diverse strategies to cope with drought. As a result, divergent responses of different vegetation types for similar levels of drought severity have been observed. It remains unclear whether such divergence can be explained by different drought duration, co-occurring compounding effects, e.g., of heat stress or memory effects, management practices, etc.

Here, we provide a global synthesis of vegetation resistance to drought and heat using different proxies for vegetation condition, namely the Vegetation Optical Depth (SMOS L-VOD) data from ESA's Soil Moisture and Ocean Salinity (SMOS) passive L-band mission and EVI and kNDVI from NASA MODIS. L-VOD has the advantage over more commonly used vegetation indices (such as kNDVI, EVI) in that it provides more information on vegetation structure and biomass and suffers from less saturation over dense forests compared. We apply a linear autoregressive model accounting for drought, temperature and memory effects to characterize ecosystem resistance by their sensitivity to drought duration and temperature anomalies. We analyze how ecosystem resistance varies with land cover across the globe and investigate the modulation effect of forest management and crop irrigation. We compare estimates of ecosystem resistance to drought and heat between L-VOD, kNDVI and EVI.

We find that regions with higher forest fraction show stronger ecosystem resistance to extreme droughts than cropland for all three vegetation proxies. L-VOD indicates that primary forests tend to be more resistant to drought events than secondary forests, but this cannot be detected in EVI and kNDVI. The difference is possibly related to EVI and kNDVI saturation in dense forests. In tropical evergreen broadleaf forests, old-growth trees tend to be more resistant to drought than young trees from L-VOD and kNDVI. Irrigation increases the drought resistance of cropland substantially. Our results suggest that ecosystem resistance can be better monitored using L-VOD in dense forests and highlight the role of forest cover, forest management and irrigation in determining ecosystem resistance to droughts.

https://doi.org/10.5194/egusphere-2023-304
Preprint. Discussion started: 28 March 2023

1 Introduction

Heat waves and drought events have become more frequent since the last century and this trend is expected to continue across many regions under projected environmental changes with high confidence (IPCC, 2021). These events disturb ecosystems and can potentially weaken the land carbon sink (Schwalm et al., 2012; Reichstein et al., 2013; Zhang et al., 2019). During the past decade, the negative effects of climate variability and change contribute to a decline in the land sink in tropical forests across Amazonia and counterbalanced the CO2 effects in many regions (Friedlingstein et al., 2022). However, drought impacts differ among ecosystems depending on the ability of ecosystems to maintain their functioning during adverse conditions, i.e., the ecosystem resistance and the recovery trajectory following the disturbance (Ingrisch and Bahn, 2018; Gessler et al., 2020). The mitigation of climate extreme events and maintenance of land carbon sink are highly dependent on the resistance of ecosystems and their changes under land use and land cover change.

Ecosystem resistance to drought stress may vary with ecosystem composition. Experimental and site-based studies have compared the growth decline and mortality rate between different plant species and functional types during drought events. Gymnosperms show higher hydraulic safety margins than angiosperms, suggesting a higher tolerance to drought stress (DeSoto et al., 2020). On the other hand, higher biodiversity has been found to strengthen ecosystem resistance to drought events in temperate beech and thermophilous deciduous forests in drought-prone environments (Grossiord et al., 2014) and in grassland with stabilized ecosystem productivity (Isbell et al., 2015). However, previous studies provide only regional results. Furthermore, inconsistency in definitions of ecosystem resistance, considered drought duration (Slette et al., 2019), measurement time and frequency between plots make the samples available for comparison limited.

To achieve a broader coverage and make consistent comparisons, satellite products (e.g., EVI, NDVI, VOD) and dynamic global vegetation models (DGVMs) are used to evaluate the ecosystem response during drought extreme events. With NDVI, Liu et al. (2022) have found an enhanced drought resistance from tree species diversity in dry forests such as xeric woodland, subtropical dry forests and Mediterranean forests. Taller tropical forests have been shown to be more vulnerable to droughts because of smaller xylem-transport safety margins based on Ku-band VOD (Liu et al., 2021b). However, these satellite products are less capable of detecting vegetation dynamics in dense forests. NDVI and EVI show saturation in dense forests (Li et al., 2021). kNDVI is better correlated with key vegetation parameters, such as leaf area index (LAI), gross primary productivity (GPP), and sun-induced chlorophyll fluorescence (SIF). It shows a higher resistance to saturation (Camps-Valls et al., 2021), but the signal still reflects mostly the upper canopy layer and cannot detect biomass changes below the canopy. For complex ecosystems with a multi-layer structure, e.g., the Amazon rainforest, the impacts cannot be detected from observations of the top canopy greenness (Walther et al., 2019). Several studies have investigated the sensitivity of GPP to drought events (Bastos et al., 2020; Flach et al., 2018; Zscheischler et al., 2014). DVGMs and upscaled FLUXCOM GPP have suggested that GPP anomalies are less negative or even positive for pixels including more than 80%

https://doi.org/10.5194/egusphere-2023-304
Preprint. Discussion started: 28 March 2023

forest cover, but under the same negative soil moisture anomaly, and pixels with higher crop cover show stronger negative impacts (Bastos et al., 2020). However, ecosystem fluxes are not directly observable at the ecosystem scale. Biomass changes, on the other hand, can be retrieved globally from satellite data, being therefore useful to quantify the ecosystem resistance worldwide.

The majority of the land surface is managed by humans. By changing the biophysical and biogeochemical properties of the land surface and the plant functional traits, management practices also affect ecosystem resilience to climate extremes. For example, modifying forest density and structure by high-intensity overstory removal was tested in conifer-broadleaf mixed forests in Central Europe and considerably increased their growth resilience to droughts and decreased drought-induced mortality by two-thirds (Zamora-Pereira et al., 2021). For cropland, irrigation has been proven to be an effective strategy to mitigate the impacts of heat waves and drought events (Jia et al., 2019). Aside from directly alleviating soil water deficits and mitigating drought impacts, irrigation of land causes a global increase in evaporation of 32500 $m^3 s^{-1}$ (Sherwood et al., 2018) and a decrease in mean surface daytime temperature (Mueller et al., 2016). Such cooling can locally mitigate the effect of heat waves. The dependence of ecosystem resilience on tree species, height, size, age and land cover types also suggests that land management related to the above parameters may strongly affect the ecosystem response to extreme events (Condit et al., 1995; Nepstad et al., 2007; McDowell et al., 2008; McDowell and Allen, 2015; Liu et al., 2021a, b). Nevertheless, there is a lack of studies linking forest management to ecosystem resistance at a global scale. With the projected increased intensity and frequency of droughts and heat extremes in the coming decades, it is important to evaluate the role of various land management practices on the resistance and resilience of ecosystems to those events.

Aiming at a global analysis of ecosystem resistance based on ecosystem state variables, we use the L-band passive microwave observations of Vegetation Optical Depth (L-VOD) from the Soil Moisture and Ocean Salinity (SMOS) satellite, which can be related to aboveground biomass at annual timescales (Brandt et al., 2018; Fan et al., 2019; Qin et al., 2021). As a comparison, we also use EVI and kNDVI. Specifically, we use global L-VOD spanning from 2010 to 2020 to investigate the spatial variability of ecosystem resistance to heat and drought events. Ultimately, we explore several possible effects of land cover and land management, including dominant vegetation cover, forest fraction, irrigation areas, and forest ages on the spatial variability of ecosystem resistance to heat and drought events.

2 Data and Methods

2.1 Satellite data

Table 1 presents an overview of the vegetation datasets included in this study. We used vegetation optical depth (VOD) data from the SMOS low-frequency microwave satellite (SMOS L-VOD) as an indicator of vegetation dynamics (Wigneron et al., 2021). Vegetation optical depth (VOD) parameterizes the attenuation of the microwave radiation when passing through

https://doi.org/10.5194/egusphere-2023-304
Preprint. Discussion started: 28 March 2023

the vegetation layer accounting for the effects of both the woody and leafy components of the vegetation canopy. VOD varies with both the mass of water contained in the canopy and the canopy structure. Different VOD datasets have been interpreted to be dominantly sensitive to vegetation biomass at an annual scale, based on the assumption that relative water content (RWC) in vegetation is stable from year to year (Brandt et al., 2018). Therefore, VOD has been used as a proxy for biomass (Brandt et al., 2018; Fan et al., 2019). Since it is independent of any vegetation index, VOD is robust for application in ecology and climate change studies. Compared to traditional vegetation indices (NDVI, EVI) and Ku-VOD, X-VOD, C-VOD, L band VOD (L-VOD) is less sensitive to saturation effects at high biomass densities and considers the entire canopy, not just the top layer as for high-frequency VOD (Fan et al., 2019).

Table 1. Overview of the satellite products included for investigating vegetation dynamics.

Variable	Dataset	Metadata period	Sampling (time, space)	Reference
SMOS L-VOD	SMOS	2010-2020	Monthly, 0.25º	(Wigneron et al., 2021; Yang et al., in review, Nat. Geo)
NDVI	MODIS	2000-2020	16-day, 0.05º	(Didan, 2015)
EVI	MODIS	2000-2020	16-day, 0.05º	(Didan, 2015)

The product of L-VOD for the period of 2010–2021 afterwards was filtered strictly (Yang et al., in review), in order to remove the effects of radio frequency interference (RFI) on signals in some regions of the northern hemisphere. The strictly filtered L-VOD data with good quality then were reconstructed using a curve-fitting method used for CO2 measurements (Thoning et al., 1989). The specific process is as follows: First, the L-VOD data were fitted using both a harmonic function (reflecting seasonal cycle) and a polynomial function (reflecting long-term variability). Second, the residuals of the fitting were further transformed using a Fast Fourier Transform, and then filtered using low pass filters, to track the remaining seasonal oscillation and long-term variations. The reconstructed L-VOD data can be separated into two time series including the long-term variability only and the seasonal oscillation only. The former mainly reflects vegetation carbon dynamics, while the latter is more affected by the seasonality in the vegetation water content.

SMOS L-VOD data are more complex to interpret when the ground is frozen (e.g., ice, snow), hence, we removed observations where the MODIS snow or ice cover fraction in the specified pixel is larger than zero. We also filtered out observations where the MODIS vegetation cover fraction is less than 0.05 to focus on vegetated land pixels. L-VOD is also sensitive to the moisture content of vegetation, which may be altered by water stress (Konings et al., 2021). Wigneron et al. (2020) proposed that the yearly average of the moisture content of vegetation is roughly constant between years at a 25 km

https://doi.org/10.5194/egusphere-2023-304
Preprint. Discussion started: 28 March 2023

scale. To limit the impact of variations in water content in estimates of vegetation resistance, we used the yearly maximum VOD as a proxy of the annual biomass that occurs mostly in the wet month, because relative vegetation water content during wet months is likely to be relatively stable over 2010–2021 so that the annual maximum L-VOD changes are closely related to vegetation biomass changes (Qin et al., 2021). This method resulted in 11 yearly values of L-VOD from 2010 to 2020.

Two optical vegetation indices, NDVI and EVI data acquired from the Moderate Resolution Imaging Spectroradiometer (MODIS) instrument aboard the Terra satellite were used to compare with the SMOS L-VOD product. The MODIS-derived NDVI and EVI datasets are temporally and spatially consistent as they are obtained from a single platform and sensor and are regarded as state-of-art proxies for green vegetation cover. We further calculated kNDVI, a nonlinear generalization of the NDVI following Eq. (1):

$$kNDVI = tanh(NDVI^2)\ , \quad (1)$$

kNDVI has been shown to perform better than NDVI and NIRv with stronger correlations with flux tower estimates of gross primary productivity and satellite retrievals of sun-induced fluorescence. It has been evaluated to be more resistant to saturation and noise (Camps-Valls et al., 2021). Compared to NDVI, EVI is proposed to decouple the canopy background signals and reduce the atmospheric influence. It presents higher resistance to saturation over dense forest areas (Zeng et al., 2022).

2.2 Climate drivers

The climate variables were acquired from the ERA5 reanalysis product at 0.25º spatial resolution for the 1979–2020 period (Hersbach et al., 2020) (https://cds.climate.copernicus.eu/cdsapp#!/home). To assess the ecosystem sensitivity to droughts and temperature, we used monthly averaged volumetric soil water in four soil layers at depths of 0–7, 7–28, 28–100, and 100–289 cm, and 2 m air temperatures. We calculated total soil moisture (SM) using the depth-weighted average of the volumetric soil water in the four layers.

Drought severity was quantified using the probability P(x< SM) of the kernel density estimate (KDE) fitted using the distribution of monthly total SM anomalies for the 1979–2020 time period. We used KDE to fit the distribution (Flach et al., 2018). The total SM anomalies were then linearly detrended and deseasonalized. A given month t was defined as a drought month when P(x < SM anomalies t) < 0.1 (monthly SM anomalies are less than the 10th percentiles of the KDE fit).

2.3 Land cover and land management data

Given the uncertainties in the land-cover mapping (Hartley et al., 2017; Li et al., 2018), we used three global land cover maps in our study presented in Table 2. These were resampled from their original resolution to 0.25º spatial resolution for the 2010–2020 period to match the spatial resolution of L-VOD.

https://doi.org/10.5194/egusphere-2023-304
Preprint. Discussion started: 28 March 2023

Table 2. Overview of the land cover products included in this study.

Land cover	Metadata period	Sampling	Reference
MCD12Q1	2001-2020	Yearly, 500m	(Friedl, 2019)
Land Cover CCI	1992-2020	Yearly, 300m	(ESA, 2022)
LUH2 v2h	850-2100	Yearly, 0.25º	(Hurtt et al., 2020)

We derived land cover classification based on the International Geosphere-Biosphere Program (IGBP) scheme from MODIS land cover map. ESA Land Cover CCI product and LUH2 v2h use different land cover classifications. The ESA Land Cover CCI product provided 37 classes based on the United Nations Land Cover Classification System (UN-LCCS; Di Gregorio and Jansen, 2005). These were then converted to 14 plant functional types (PFTs) using the lookup table in Poulter et al. (2015). To better account for the intrinsic bias and classification differences among the three products, we further aggregated the original classes into four biomes (forests, shrublands, grasslands and croplands) according to Table 3. We categorized land cover in bins of 25% fraction of each biome and, for each pixel, assigned the land cover information with the highest agreement across datasets (>= 2 agree). To guarantee that our results are not biased by the land cover change (e.g., deforestation), we excluded those pixels showing changes in the 25% bins during 2010–2020.

The LUH2 v2h dataset also provides land management information, for example, forested primary land and potentially forested secondary land (Figure 1). We also used the global map of irrigation areas around 2005 at 0.0833º spatial resolution from FAO (Siebert et al., 2013). The latter map provides areas equipped for irrigation as the percentage of total grid cell area (f_e) and the percentage of area equipped for irrigation that was actually irrigated (f_a), based on national census surveys or irrigation sector studies. We then assumed that the irrigation equipment is totally located in cropland and calculated the percentage of cropland actually irrigated f_{ac} as f_a*f_e/f_c, where f_c is cropland percentage of grid cell area (Figure 1). To explore the influence of tree characteristics on their resistance to droughts, we used a global forest age map estimated from forest inventories, biomass and climate data at 0.00833º spatial resolution (Besnard et al., 2021).

All above datasets were resampled to 0.25º to make them comparable to the relatively coarse L-VOD data. For the global forest age map, we calculate the average of the forest age in pixels at 0.25º.

https://doi.org/10.5194/egusphere-2023-304
Preprint. Discussion started: 28 March 2023

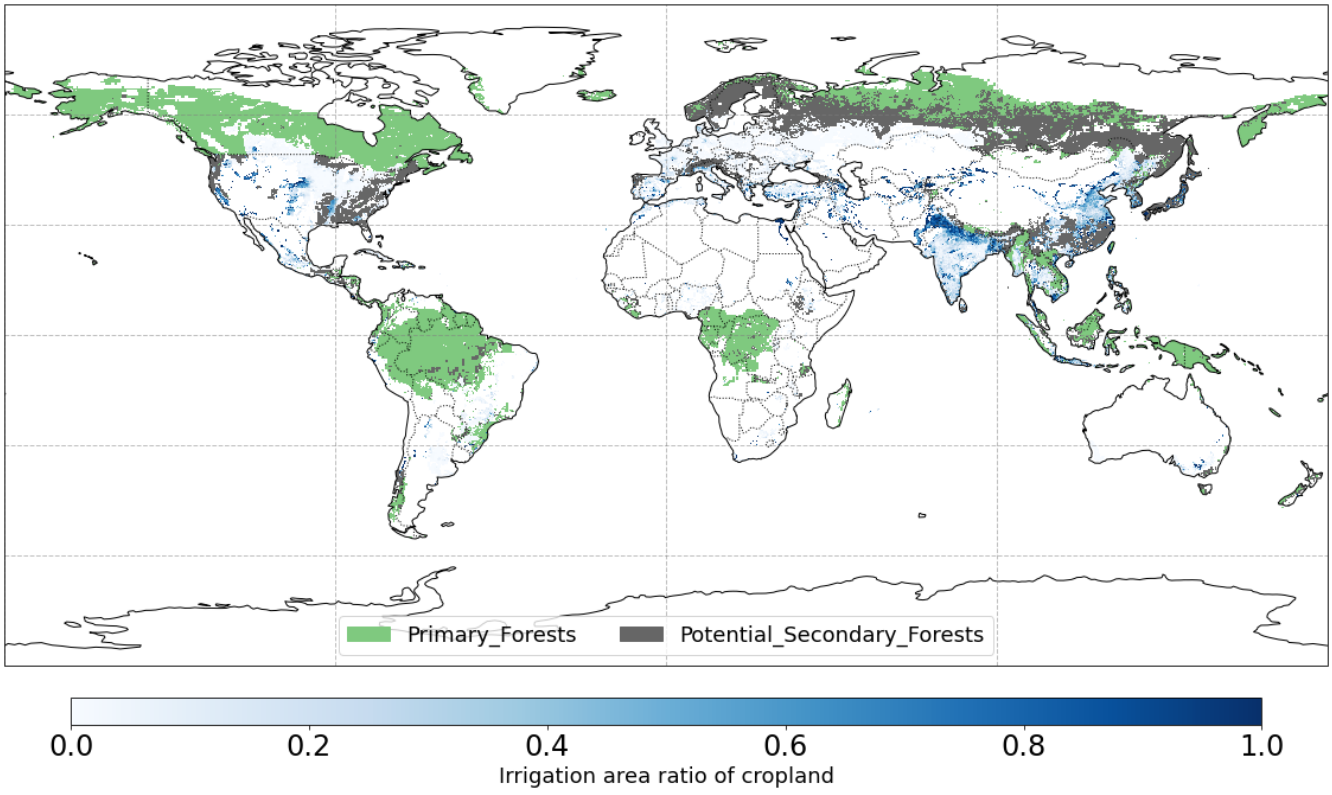

Figure 1. Global map of forest management types in LUH2v2 and irrigation area ratio of cropland for MODIS cropland >25%.

2.4 Definition of ecosystem resistance

To calculate the ecosystem resistance to heat and drought, we applied a linear autoregressive model of 1 year lag for each pixel following Eq. (2):

$$Y_{anom}(t) = \alpha N(t) + \beta T_{anom}(t) + \varphi Y_{anom}(t-1) + c + \epsilon(t)\,, \quad (2)$$

for the year t ranging from 2011 to 2020, in which Y represents either yearly maximum L-VOD, yearly mean kNDVI or EVI. N is the centered number of drought months in each year. T is the yearly mean 2 m air temperature. All anomalies were calculated through the subtraction of linear trends and through the subtraction of the average for each month over the time period 2010–2020. The anomalies were then standardized. ϵ is the residual term. The model coefficient α, also known as the sensitivity of Y to N, can be closely related to the inverse of ecosystem resistance during the drought period. We used $\alpha(month^{-1})$ as a metric for the ecosystem resistance to droughts. If α is negative, the vegetation L-VOD and greenness are negatively disturbed during the drought period. On the contrary, if α is positive, the vegetation grows better during the drought period than in normal SM conditions. Higher α indicates stronger ecosystem resistance to droughts. Similarly, we used β as a metric for the ecosystem resistance to temperature anomalies. This approach also partly controls for the

https://doi.org/10.5194/egusphere-2023-304
Preprint. Discussion started: 28 March 2023

covariance between drought and temperature. The third term of the equation corresponding to the previous year's vegetation anomalies could be associated with the recovery rate to the average state or persistent impact during the next year. Thus, φ can represent vegetation memory, which has previously been proposed to be associated with long-term resilience to any type of perturbation. α is in the unit of $month^{-1}$ but β and φ have no unit due to standardization. Therefore, we cannot directly compare α with β to assess the effect of droughts and temperature anomalies. Ecosystem resistance to droughts and temperature were evaluated for each pixel.

2.5 Statistical analysis

As described above, we characterized ecosystem resistance by the sensitivity of the vegetation state to the drought length and 2 m temperature anomalies. We further masked pixels where no droughts occurred in the 2010–2020 period. We aggregated the values of ecosystem resistance for IPCC AR6 reference sub-regions (Iturbide et al., 2020), dominant IGBP vegetation cover classes (Figure 3a), forest and cropland fraction, forest management types and irrigation percentages. We compared the distributions of these groups and distinguished the effect of increasing coverage of specific biomes or some specific land management.

As the secondary forests dominate mid latitudes and the primary forests dominate tropical and boreal regions, to minimize the potential confounding environmental effects on the results, we extracted only pairs of primary and secondary forests sharing similar long-term temperature and precipitation averages. First, the grid cells were filtered by >50% forest fraction and those containing LUH2 v2h forest management information were categorized according to ERA5 temperature and total precipitation long-term averages. Temperature is divided into 25 groups T_i (i = 1–25) from -10 °C to 30 °C uniformly and precipitation is divided into 25 groups P_j (j = 1–25) from 0 to 5000 mm uniformly, which results in 625 bins T_iP_j. Second, if there are more than 5 pixels of primary forests PF_k and 5 pixels of secondary forests SF_l in one bin T_iP_j, the difference between the average of these pixels are calculated as $\Delta T_iP_j = \overline{PF_k} - \overline{SF_l}$. We then showed the distribution of these differences for different bins ΔT_iP_j in the boxplot.

To compare the ecosystem resistance of forests with different mean ages, we filtered pixels with dominant tropical evergreen broadleaf forests and >50% forest fraction and grouped the forest ages into three groups [0, 100), [100, 300) and ≥ 300 years. We compared the crop irrigation ratio between categories < 10%, 10% to 50% and ≥ 50% for pixels with >50% cropland fraction, which is dominated by cropland in India and North America (Figure 1).

https://doi.org/10.5194/egusphere-2023-304
Preprint. Discussion started: 28 March 2023

3 Results

3.1 Contrasting patterns of ecosystem resistance to droughts and temperature over different regions and dominant vegetation types

At the global scale, the ecosystem resistance coefficient α based on the linear AR1 model are negative in 54% of pixels with valid values from EVI and L-VOD and 57% from kNDVI. (Figure 2a-2c, Figure 3a). Negative resistance values predominate in mid latitudes, while positive values are found for the boreal regions (Figure 2d). In the tropics, we find the largest divergences between the three indices, where the resistance from L-VOD is positive in Amazon, central Africa and Southeast Asia regions, but EVI shows the lowest resistance with a median of -0.028 $month^{-1}$ with an obvious disagreement with VOD with a median of 0.029 $month^{-1}$ and kNDVI with a median of 0 $month^{-1}$ in Southeast Asia regions. Ecosystem resistance from kNDVI is closer to L-VOD with a higher percentage of positive resistance in Southeast Asia. In the Amazon region, there are around 10% more pixels showing negative resistance from EVI and kNDVI than L-VOD. The standard error of the drought resistance coefficient is relatively higher for tropical regions with higher uncertainties in the edge of the Amazon and central Africa forests (Figure 2e-2h).

The ecosystem resistance to temperature shows a clearer spatial pattern. The ecosystem resistance to temperature is negative and lower in tropical regions compared to mid latitudes (Figure 2l), indicating a decline in vegetation biomass and greenness during hot weather and a weaker ecosystem resistance to high temperatures in tropical regions. In boreal regions, the ecosystem resistance is mostly positive, which indicates vegetation growth during hot weather and thus a stronger resistance to hot events. In the tropics, the forest regions and non-forest regions show divergent resistance, with forest regions showing mostly positive resistance to temperature, and negative values predominating in grassland or savannas. L-VOD shows a large deviation relative to kNDVI and EVI in boreal regions, mostly because of missing data for L-VOD in those regions. The standard error is also relatively higher for the Northern Hemisphere with higher land cover fraction but more pixels with missing values.

https://doi.org/10.5194/egusphere-2023-304
Preprint. Discussion started: 28 March 2023

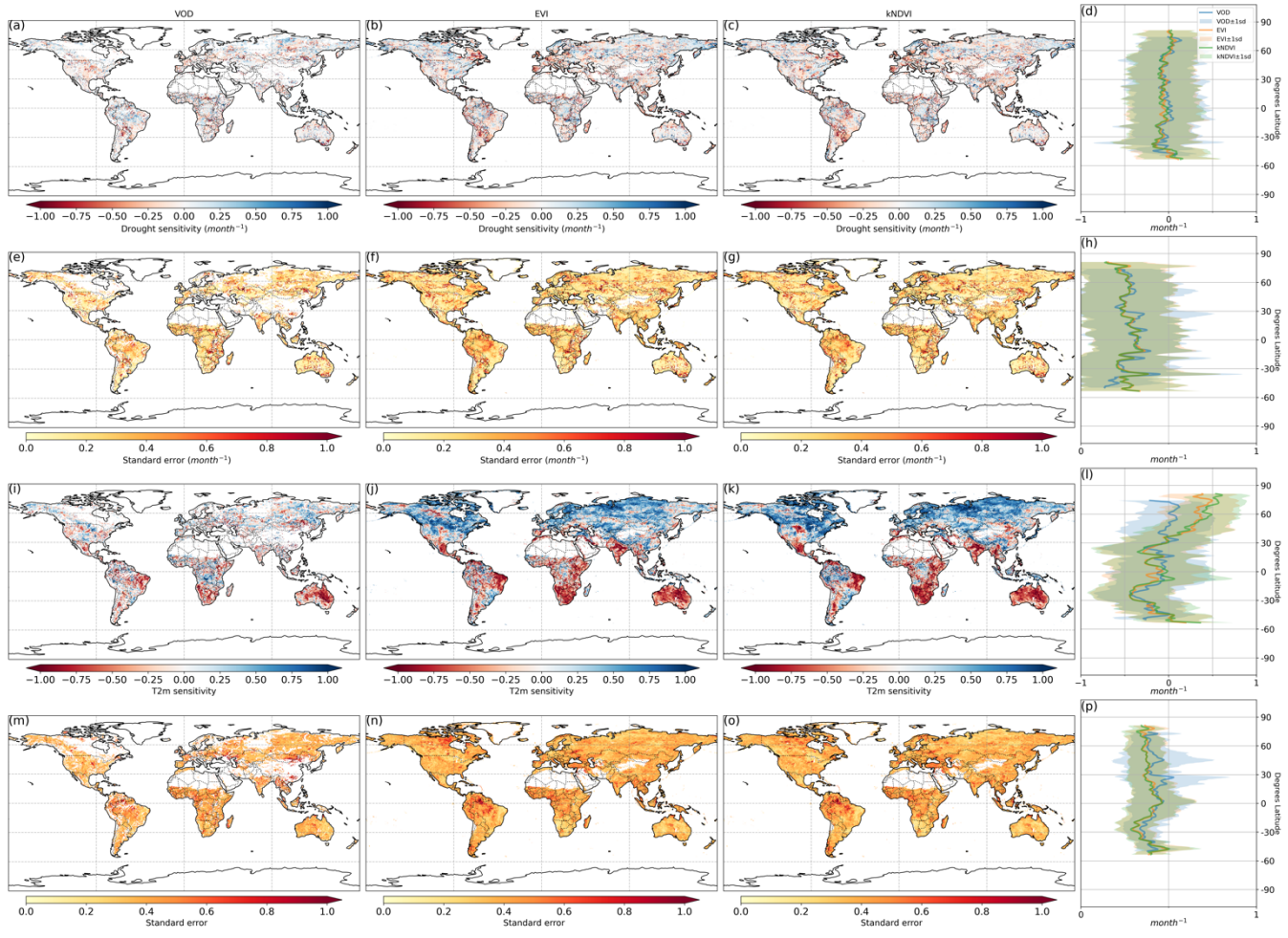

Figure 2. Ecosystem resistance to drought duration and its standard error. Spatial map of drought coefficients α for (a) L-VOD, (b) EVI, (c) kNDVI and their standard error (e, f, g). Same for temperature coefficients β (i, j, k) and their standard error (m, n, o). The averages for different latitudes and their standard deviations are shown on the right (d, h, l, p).

We summarize the results for each of the IPCC AR6 sub-regions in Figure 3. 27 regions coloured red or blue in Fig. 3a have a mean ecosystem resistance that is significantly different from zero on a two-tailed Student t-test (P-value < 0.05), the medians of ecosystem resistance range from -0.20 to 0.07 $month^{-1}$ and the averages of α range from -0.25 to 0.08 $month^{-1}$. The mean α in 20 of these regions is negative. Only NWN, NEU, RAR, and RFE in the boreal region, NSA, SAM and SEA with high forest cover fraction show positive mean α. By contrast, most regions over mid-latitudes (30°–60°) show negative mean α (Figure 3a, 3b).

In the tropics, SAS, CAF, SEAF, and NAU, which have lower forest cover show negative mean α, while NSA, SEA and SAM, which are dominated by evergreen broadleaf forests, show higher resistance and positive mean α. We grouped α by

https://doi.org/10.5194/egusphere-2023-304
Preprint. Discussion started: 28 March 2023

different IGBP vegetated land cover types from forests to cropland. Calculated from L-VOD, the ecosystem resistance to droughts is higher in shrublands (SH), evergreen needleleaf forests (ENF) and evergreen broadleaf forests (EBF) but relatively lower in deciduous needleleaf forests (DNF), deciduous broadleaf forests (DBF) and cropland (C) (Figure 3c). kNDVI and EVI agree on the lowest resistance in C and high resistance in SH, ENF, and mixed forests (MF) (Figure A3).

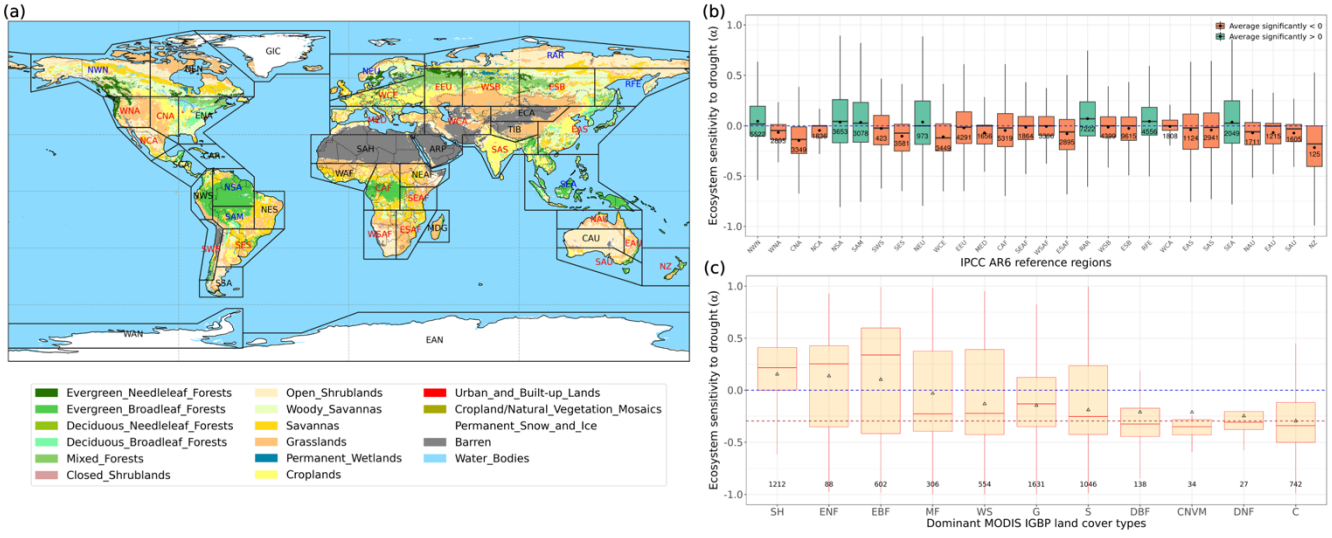

Figure 3. Regional pattern of ecosystem resistance to drought duration. (a) Distribution of the IGBP land cover types based on MODIS (MCD12Q1). The boxes with abbreviations indicate updated reference regions for IPCC AR6 WG1. Blue represents significant positive resistance and red represents significant negative resistance; (b) Distribution of ecosystem resistance α to drought for different reference sub-regions, the number in each box is the number of pixels in this category; (c) Distribution of ecosystem resistance to drought α for different dominant IGBP vegetation classes. Only significant α from the linear AR1 model is selected (P-value<0.05) and only regions with averages that are statistically different from zero are shown (two-sided Student t-test; P-value<0.05).

3.2 The importance of forest cover fraction in modulating ecosystem resistance

A given pixel can have a mixture of several land cover types with very similar fractions, but the dominant land cover pattern ignores this effect. Therefore, we further analysed mean α among different forest and crop cover fractions. In general, the mean α is lower (more negative) with decreasing forests and increasing cropland fraction. Pixels dominated by forests (indicated by the green box) are significantly more resistant to droughts than those where cropland predominates (Figure 4a-c). The ecosystem resistance α increases from a mean of -0.18 $month^{-1}$ to 0.09 $month^{-1}$ with increased forest fraction and decreases from -0.27 $month^{-1}$ to -0.36 $month^{-1}$ with increased cropland fraction. The resistance is close to zero because pixels with less than 25% forest and less than 25% cropland are dominated by low-vegetated land or bare soil, so that the signal of vegetation is weak.

In forest-dominated regions (>50% forest fraction), the difference between results for L-VOD, EVI and kNDVI becomes more obvious than in crop-dominated regions. Ecosystem resistance is the highest and even positive for L-VOD and the lowest for EVI, and kNDVI shows similar ecosystem resistance to that of L-VOD.

https://doi.org/10.5194/egusphere-2023-304
Preprint. Discussion started: 28 March 2023

The contrast between forest-dominated regions and crop-dominated regions also exists for ecosystem resistance to 2 m air temperature from EVI and kNDVI (Figure 4e-f). The significant positive sensitivity to temperature predominates in the regions with more than 25% forests while the sensitivity is negative in the regions with more than 50% cropland. The pattern is distinct for different climate zones and shows strong latitudinal dependence. For tropical regions, except for kNDVI in a small fraction of regions, most ecosystems show negative resistance to temperature, which means that higher temperatures lead to a negative impact over a large area in the tropics (Figure A5a-c). In temperate climate zones, predominant in mid latitudes, all three vegetation products agree on the negative resistance in the regions with less than 25% forest cover, but NDVI and EVI show a higher positive resistance in the regions with more than 25% forest cover (Figure A5d-f). In the boreal region, the resistance values are generally positive (Figure A5g-i), which confirms the variability of resistance to temperature to latitudes.

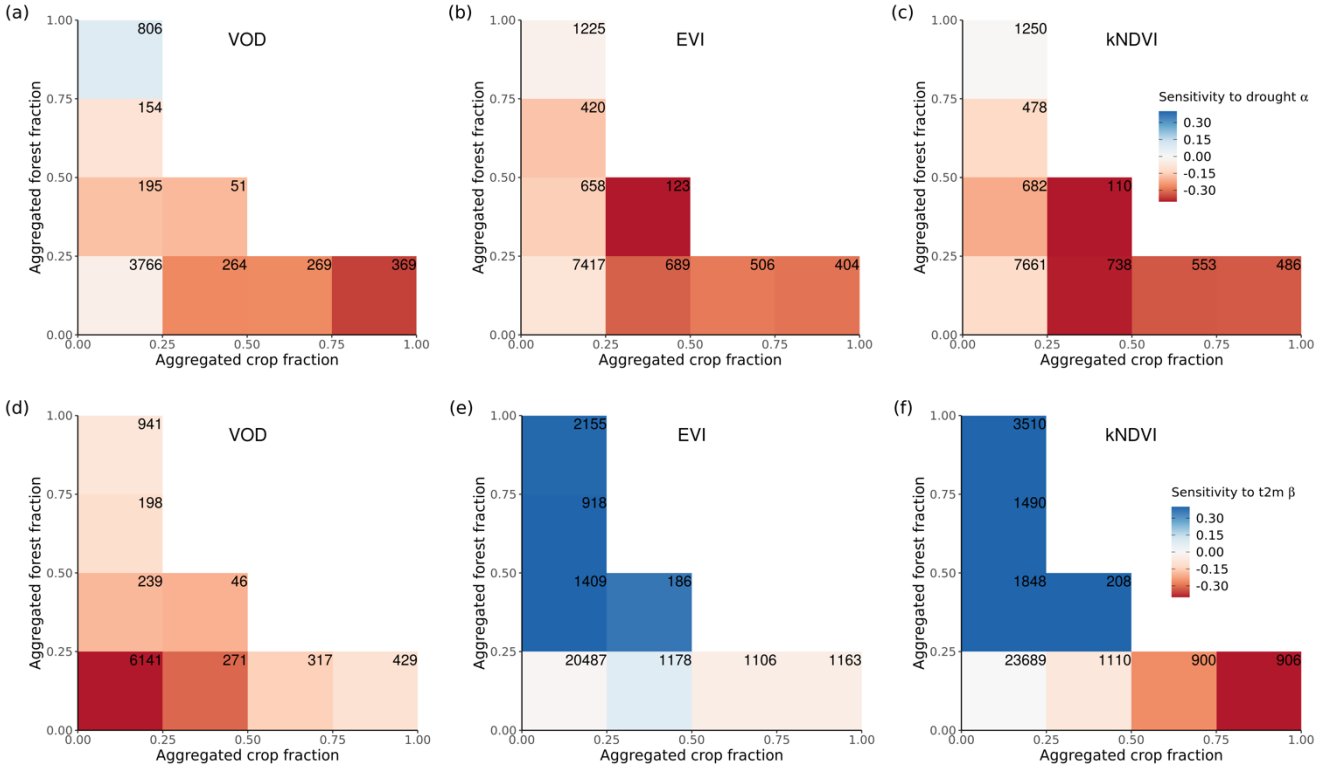

Figure 4. Ecosystem resistance to drought and temperature binned for different levels of the aggregated forest and cropland fraction classes from the three land cover products (a) L-VOD, (b) EVI and (c) kNDVI for drought resistance coefficients α and (d-f) for temperature resistance coefficients β. Only significant coefficients α in the linear AR1 model (P-value<0.05) are included and groups with less than 20 pixels are excluded. The number in each bin is the number of pixels in this category.

https://doi.org/10.5194/egusphere-2023-304
Preprint. Discussion started: 28 March 2023

3.3 The roles of forest management, crop irrigation and forest ages in modulating ecosystem resistance

The above results suggest that a transition between dominant vegetation types modifies ecosystem resistance. Other anthropogenic disturbances, such as forest management, have the potential to influence the ability of forest ecosystems to maintain their functioning during drought-heat extremes by directly affecting tree species, age distribution, cover density, rooting depth and primary productivity. For croplands, irrigation is also an essential element to maintain and increase yields during droughts.

To detect such effects, we analysed ecosystem resistance to droughts α for primary and potential secondary forests from the LUH2 v2h land cover dataset (Figure 5a). The comparison between primary and potential secondary forests shows that the averaged ecosystem resistance α calculated from L-VOD is significantly higher in primary forests than in secondary forests. The median of the difference between primary and secondary forests $\Delta\alpha$ is 0.245 $month^{-1}$ and is significantly greater than 0 from the one-sample Wilcoxon test (P-value < 0.05). However, we did not detect such a large difference between EVI and kNDVI, whose medians of $\Delta\alpha$ between forest types are 0.033 $month^{-1}$ and 0.100 $month^{-1}$, but given the large spread of the distribution, their medians are not significantly greater than 0 based on the one-sample Wilcoxon test (P-value < 0.05).

We further tested the effect of forest ages in modulating the ecosystem resistance in the tropical evergreen broadleaf forest. From L-VOD, forests older than 100 years are substantially more resistant to drought than forests younger than 100 years. The median of ecosystem resistance α of forests younger than 100 years is -0.374 $month^{-1}$ but the medians of α of forests from 100 to 300 years and forests older than 300 years are 0.395 $month^{-1}$ and 0.375 $month^{-1}$ respectively. We also find a significant (P-value < 0.05) increase of α in kNDVI but the effect is not as large as in L-VOD. The ecosystem resistance α calculated from EVI does not show a large divergence between forests older than 300 years and forests younger than 100 years.

We finally investigated the ecosystem resistance α for different irrigation levels (Figure 5c). The result shows a consistently increasing resistance for L-VOD and EVI with the irrigation levels, with the median of α for L-VOD increasing from -0.36 $month^{-1}$ to -0.17 $month^{-1}$ and from -0.35 $month^{-1}$ to 0.25 $month^{-1}$ for EVI for irrigation levels varying between less than 10% actually irrigated cropland and more than 50% actually irrigated cropland. For kNDVI, the change in the median of α is negligible but we still found a higher percentage of pixels with close to zero or positive resistance for higher irrigation fractions.

https://doi.org/10.5194/egusphere-2023-304
Preprint. Discussion started: 28 March 2023

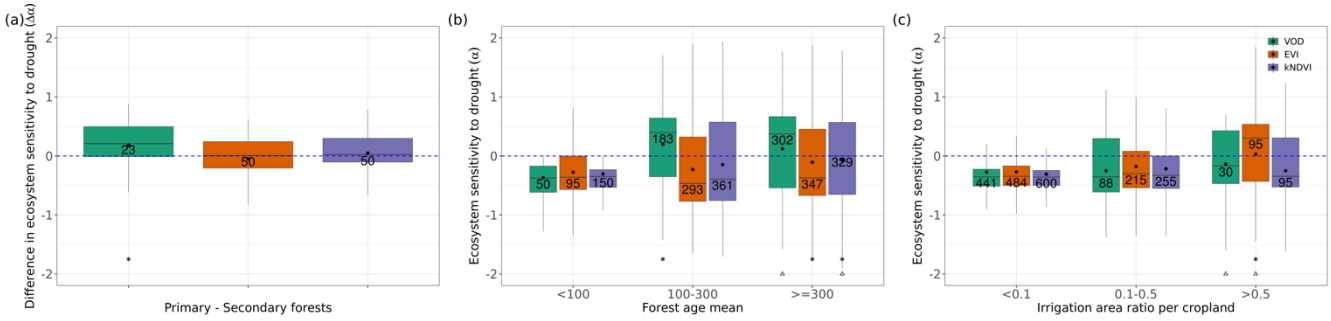

Figure 5. Ecosystem resistance to droughts for (a) forest management located in a similar background climate, and for different levels of (b) forest ages in the tropical EBF (c) crop irrigation. Only significant coefficients α in the linear AR1 model (P value<0.05) are included. Stars in (a) indicate the median value of this category is greater than 0 at the 0.05 significance level from the one-sample Wilcoxon test. Stars indicate the median value of this category is greater than the median of the previous category and triangles indicate the median of this category is greater than the median of the first category at the 0.05 significance level from the unpaired two-sample Wilcoxon test. The number in each box is the number of bins/pixels in this category.

4 Discussions

4.1 Spatial variability of ecosystem resistance to drought and temperature

Ecosystem resistance during a disturbance phase plays a key role in determining resilience. In this study, we evaluated the ecosystem resistance to drought and temperature with their sensitivity to 10th percentile soil moisture drought duration and temperature anomalies at 2 m in a linear model with an AR1 term. The IPCC AR6 sub-regions whose averages of drought resistance are significantly negative mainly correspond to semi-arid regions with high coverage of grassland, cropland and savannas and temperate deciduous forests (Figure 3a). In these semi-arid regions dominated by grassland, cropland and savannas, vegetation dynamics is more sensitive to water availability and therefore is more impacted by drought events (Poulter et al., 2014; Ahlström et al., 2015; Walther et al., 2019). In temperate forests over mid latitudes, previous studies have suggested that short seasonal droughts are more likely to induce dieback of broadleaved deciduous angiosperm trees (e.g., DBF in Fig. 3c) than conifer trees (i.e., ENF in Fig. 3c) because of the higher vulnerability to xylem cavitation of angiosperm trees (Maherali et al., 2004; Allen et al., 2010). On the contrary, the areas with significantly positive resistance to drought correspond to the dense tropical evergreen broadleaved forests and boreal continental regions with shrublands and evergreen needleleaved forests. For the boreal regions, the soil is generally humid, so that the drought defined as the 10th percentile likely still provides critical water storage for vegetation. The potential environmental limitations to vegetation growth in these areas are temperature and radiation rather than water availability (Boisvenue and Running, 2006).

The resistance to temperature highly depends on latitude. For extratropical regions, vegetation L-VOD and greenness normally increase with higher temperatures. Warming generally leads to an earlier growing season onset and results in increased early-season vegetation productivity (Forkel et al., 2016). Although we removed the confounding effect of extreme

https://doi.org/10.5194/egusphere-2023-304
Preprint. Discussion started: 28 March 2023

soil water deficit from L-VOD, this trend can still be adversely affected by climate variability and other emerging limitations from energy and nutrients on vegetation production (Piao et al., 2017; Buermann et al., 2018; Liu et al., 2019).

4.2 Contrasting ecosystem resistance to drought and temperature in forests and cropland

Forests and cropland respond differently to extreme drought events. Ecosystem resistance increases with increased forest and decreased cropland fraction. This is also observed in previous studies based on GPP datasets over Europe (Zhang et al., 2016; Bastos et al., 2020) and SIF (Walther et al., 2019). The increasing pattern in L-VOD for dominant forests might be a result of increased insolation and photosynthetic activity light, and weak changes in greenness during the drought period (Zhu et al., 2018; Walther et al., 2019). Besides, the light use efficiency (LUE) decreased less with lower soil moisture contents in forests compared to non-forest vegetation, which could be linked to deeper and more extensive root systems with higher access to available soil water (Walther et al., 2019). The pattern is consistent for the tropical, temperate and continental climate regions except for results from EVI in the temperate climate (Figure A4) and can be explained by the intrinsic structural and physiological differences between trees and crops, for example, the deeper rooting depth of trees (Canadell et al., 1996), higher water storage capacity in the stems for forests (Matheny et al., 2015) and different water use strategies between forest and grass-/cropland (Teuling et al., 2010).

Compared to drought resistance, the ecosystem resistance to temperature shows a weaker contrast in L-VOD between forests and cropland, instead, latitude dependence plays a more important role here (Figure A5). Nevertheless, from EVI and kNDVI, we still observe a divergent response to temperatures between forest-dominated regions and crop-dominated regions in tropical and temperate climate zones. In the temperate regions, forests may benefit from higher temperatures through warming-induced changes in their phenology, while crops might show a nonlinear response of photosynthesis to temperature, due to a weaker resistance to hot extreme days. A strong trend of earlier spring growing season onset and later autumn senescence has been observed in the temperate forests in the eastern USA (Keenan et al., 2014). In boreal climate zones in the Northern Hemisphere, L-VOD, EVI and kNDVI generally show a strong positive relationship with an increase in temperature, which can be interpreted as an increase in photosynthesis in response to warming (Piao et al., 2006).

At the same time, croplands can be affected by different management practices, for example, crop rotation that changes from year to year and the variable timing of planting and harvesting also has an influence on vegetation biomass. By taking the yearly maximum L-VOD value, we partly alleviate such an influence and expect interannual variations to better correspond to biomass changes.

4.3 Modulation by land management and forest age in ecosystem resistance

After accounting for the potential effect of climate background, the primary forest still shows significantly higher resistance than the potential secondary forest from L-VOD (Figure 5a). The pixel number is different due to a different ratio of

https://doi.org/10.5194/egusphere-2023-304
Preprint. Discussion started: 28 March 2023

significant resistance for primary and secondary forests located in similar climate backgrounds. Primary forests have substantially higher biodiversity values compared to secondary degraded forests even after partly accounting for confounding colonization and succession effects from the isolation, composition of surrounding habitats, and time since disturbance (Gibson et al., 2011). High tree species diversity helps strengthen the ecosystem resistance to droughts (Liu et al., 2022). Besides, primary forests might have a more extensive rooting system than secondary forests with higher availability of soil water.

Apart from the modulation effect from land cover due to different sensitivity to drought stress for different vegetation types, at the ecosystem scale, we illustrate that over tropical EBF, older trees tend to be more resistant to droughts (Figure 5b). Young trees sometimes exhibit high drought-induced mortality rates due to limited rooting depth (McDowell and Allen, 2015). Young fast-growing and light-wooded trees are recorded to be especially vulnerable to drought by cavitation or carbon starvation (McDowell et al., 2008; Phillips et al., 2009). Older mature forests could develop a more complex ecosystem with higher species diversity (e.g., Amazon rainforest). Tree species diversity may enhance the drought resistance in global forests with a stronger effect over tropical forests (Liu et al., 2022).

Irrigation helps attenuate drought impacts and enhance the cropland resistance to drought extremes. This effect is also reflected in SIF and GPP anomalies (Gampe et al., 2021; Cheng et al., 2022). It increases the mean SM during drought events and alleviates drought-heat stress through an increase in total evapotranspiration because it will increase atmospheric water vapour amount and decrease the mean surface daytime temperature (Mueller et al., 2016).

4.4 Ecosystem resistance difference between kNDVI, EVI and L-VOD

L-VOD responds differently to drought stress with EVI and kNDVI, especially in dense forests. As shown in Figure 4, the mean of ecosystem resistance is closer for dominant cropland but differs more for the dominant forests for the three products. Similarly, enhanced ecosystem resistance is not detected in kNDVI and EVI for primary forest (Figure 5a), which is supposed to be denser with a more complex canopy structure than secondary forest. Such discrepancies can be related to the intrinsic difference in measurements between L-VOD and traditional vegetation indices. L-VOD was produced using low-frequency microwave observations. It has superior sensitivity to carbon density than NDVI, EVI and other higher-frequency VOD products with the ability to penetrate into vegetation with multi-layer canopy and upper part of stem biomass (Rodríguez-Fernández et al., 2018; Tian et al., 2018; Fan et al., 2019; Wigneron et al., 2020). As a result, it is able to retrieve the overall biomass in dense tropical ecosystems when EVI, NDVI and high-frequency L-VOD saturate (Liu et al., 2015). kNDVI overcomes the greenness saturation with increased forest cover empirically but still cannot detect the biomass change under the top canopy layer and other than leaf biomass. In dense forests, L-VOD is also sensitive to woody biomass but EVI and kNDVI only detect the top-layer canopy greenness dynamics. The correlation between L-VOD and kNDVI is also much lower in forests than in cropland and grassland (Figure 6). This is also confirmed in the difference

https://doi.org/10.5194/egusphere-2023-304
Preprint. Discussion started: 28 March 2023

between L-VOD and EVI, kNDVI in dense forests under the tropical climate (Figure A4a-c), where forest canopy structure is generally more complex with higher mean canopy. However, the ecosystem resistance to droughts is similar for dominant forests under continental climate (Figure A4g-i) because the forest canopy structure is generally simple and the forest canopy height is lower.

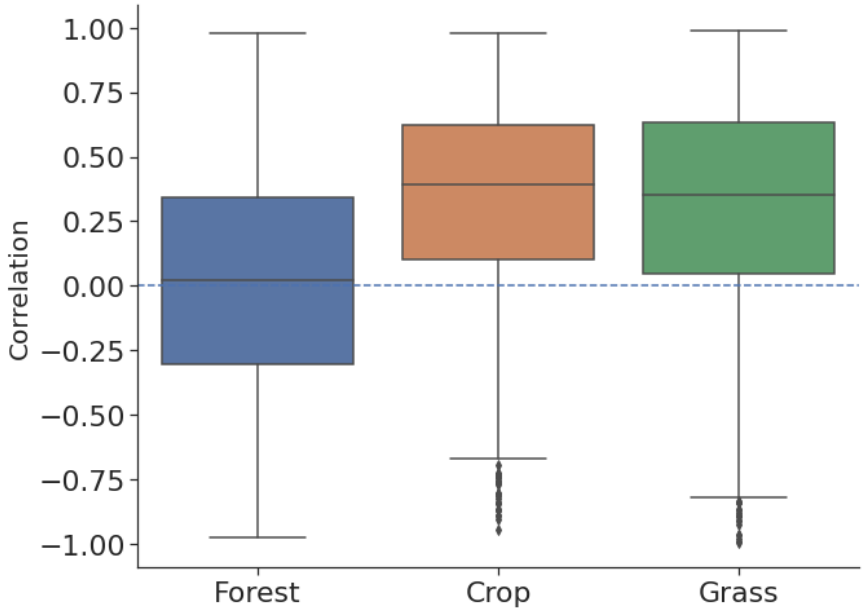

Figure 6. Correlation between yearly maximum L-VOD and kNDVI for different land cover types.

4.5 Limitations and outlook

Our method assumes a close relationship between L-VOD and vegetation biomass at an annual scale, as other studies using VOD products (Tian et al., 2017; Brandt et al., 2018; Fan et al., 2019; Wigneron et al., 2020; Qin et al., 2021). This assumption is questioned by Konings et al. (2021) and they showed a weak temporal correlation between biomass anomalies calculated from a new biomass dataset from Xu et al. (2021) and L-VOD anomalies. Yet, the ability of the new dataset to represent the inter-annual variability of biomass has not been tested. Several studies also reported a strong near-linear relationship between L-VOD and biomass for woody vegetation independent of the year (Rodríguez-Fernández et al., 2018; Brandt et al., 2018), indicating a relatively constant RWC. In our study, we used the annual maximum L-VOD values in order to minimize potential confounding effects by variations in vegetation water content. The comparison between primary and secondary forests from yearly maximum L-VOD fits better with in situ studies than EVI and kNDVI (Nunes et al., 2022), which reveals the potential of L-VOD to detect vegetation dynamics, especially in dense forests. To better disentangle the effect of RWC on L-VOD, continuous biomass measurements are required.

https://doi.org/10.5194/egusphere-2023-304
Preprint. Discussion started: 28 March 2023

In general, regions showing significant negative mean values of drought sensitivity α, which indicate negative impacts on vegetation during drought period, are mostly located in water-limited regimes (Denissen et al., 2022) except for EAS with relatively small coverage of available L-VOD data and CAF which is less homogeneous. Under climate change, the widespread shift from an energy-limited regime to a water-limited regime (Denissen et al., 2022) will put more ecosystems under threat of droughts. The modulation of drought resistance by specific land cover and land management is thus important for these regions in the future. Deforestation and a transition to cropland might potentially weaken the ecosystem resistance to extreme drought events. The protection and maintenance of primary forests are also important to sustain tropical biodiversity and its high drought resistance. For cropland, a higher irrigation ratio significantly increases the ecosystem resistance, but further precise and efficient practices of irrigation for agriculture are required to avoid a waste of water resources (Shulka et al., 2019).

5 Conclusion

This study analyses how land cover and common land management practices modulate the ecosystem responses to drought and heat based on different remote sensing products, namely L-VOD, EVI and kNDVI. Areas with predominant forest cover show stronger ecosystem resistance to extreme soil droughts than those predominated by croplands. Forests do not show obvious changes in canopy greenness indices during dry conditions compared to normal conditions, while L-VOD, as a proxy for biomass, tends to show a slight increase. This is possibly because of enhanced photosynthesis activity and a smaller decline in LUE compared to crops. Distinct responses are found between primary forests and secondary forests from L-VOD. Primary forests, typically associated with higher biodiversity, tend to show stronger resistance to droughts than secondary forests. Our findings from L-VOD show that tree age potentially contributes to the difference in drought resistance in tropical EBF, with ecosystems with older trees better mitigating drought stress.

Our results show the advantage of L-VOD in detecting vegetation dynamics in dense forests where EVI and kNDVI only detect the upper leaf canopy, which can therefore be a promising approach. In summary, we found that canopy greenness correlates well with canopy biomass and photosynthesis for nonwoody vegetation, forest biomass may fluctuate when canopy greenness is relatively stable. Irrigation helps improve the ecosystem resistance for croplands. Deforestation and afforestation leading to a change in forest cover and primary forest destruction might therefore modulate regional changes in ecosystem resistance. Forest management changes forest age distribution, possibly modulating the response of forests to droughts. The effect of forest management and crop irrigation on ecosystem resistance has important implications for the monitoring and management of ecosystems under climate change.

https://doi.org/10.5194/egusphere-2023-304
Preprint. Discussion started: 28 March 2023

Appendix A: Supplementary Figures

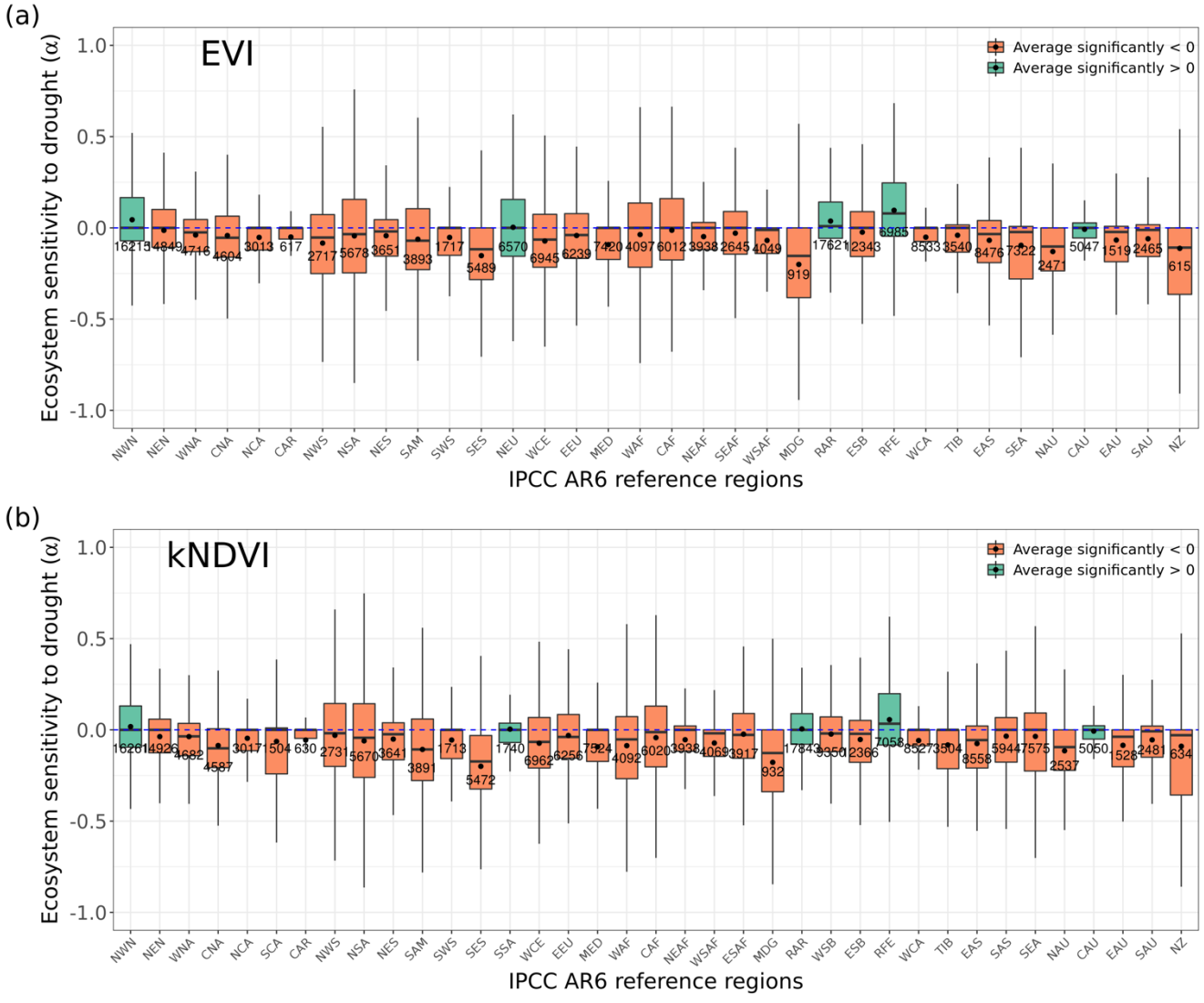

Figure A1. Distribution of ecosystem resistance α from (a) EVI and (b) kNDVI to drought for different dominant IPCC AR6 sub-regions. The boxes with abbreviations indicate updated reference regions for IPCC AR6 WG1. Blue represents significant positive resistance and red represents significant negative resistance, the number in each box is the number of pixels in this category.

https://doi.org/10.5194/egusphere-2023-304
Preprint. Discussion started: 28 March 2023

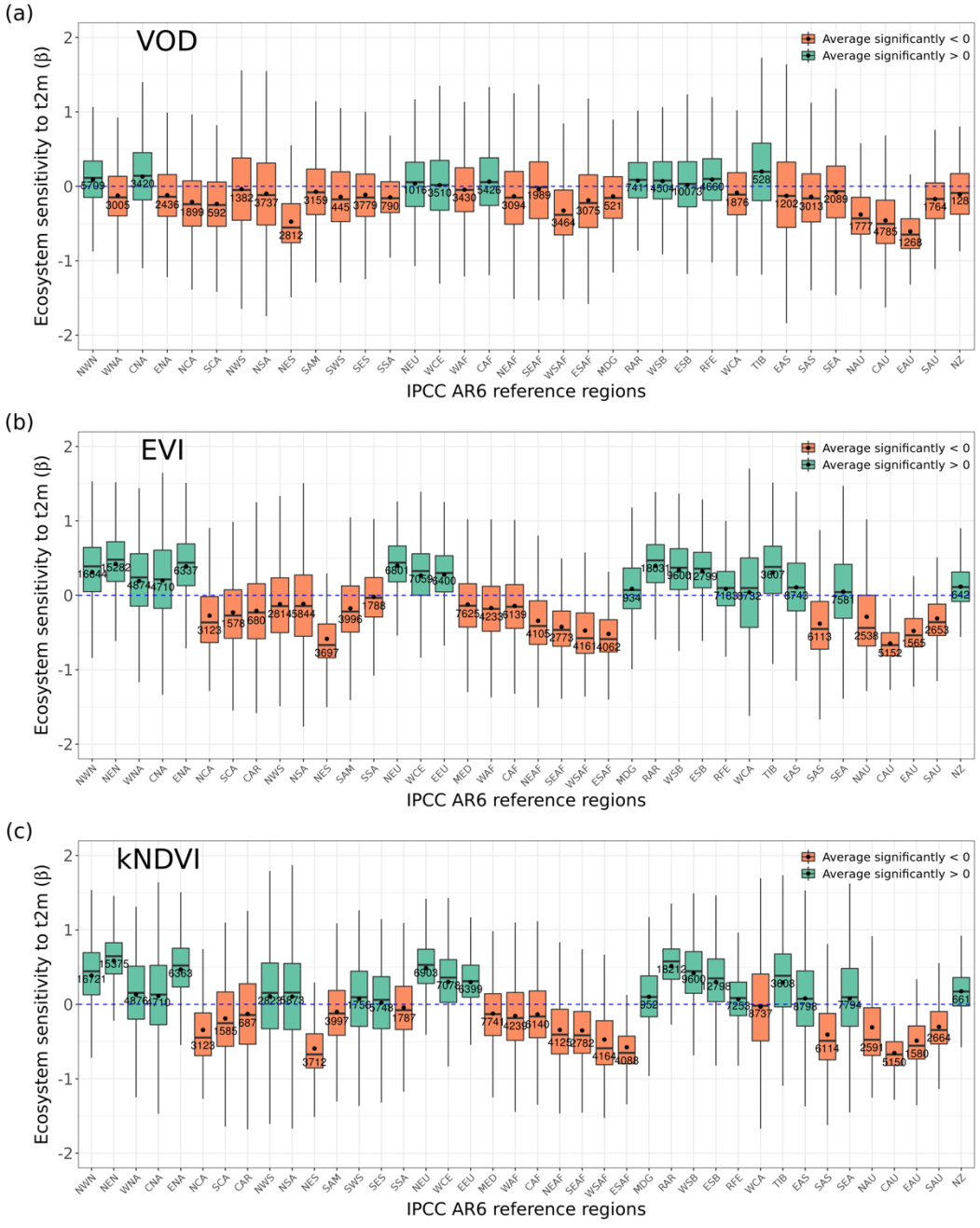

480 **Figure A2.** Distribution of ecosystem resistance to 2 m air temperature β from (a) L-VOD, (b) EVI and (b) kNDVI to drought for different dominant IPCC AR6 sub-regions. The boxes with abbreviations indicate updated reference regions for IPCC AR6 WG1. Blue represents significant positive resistance and red represents significant negative resistance, the number in each box is the number of pixels in this category.

https://doi.org/10.5194/egusphere-2023-304
Preprint. Discussion started: 28 March 2023

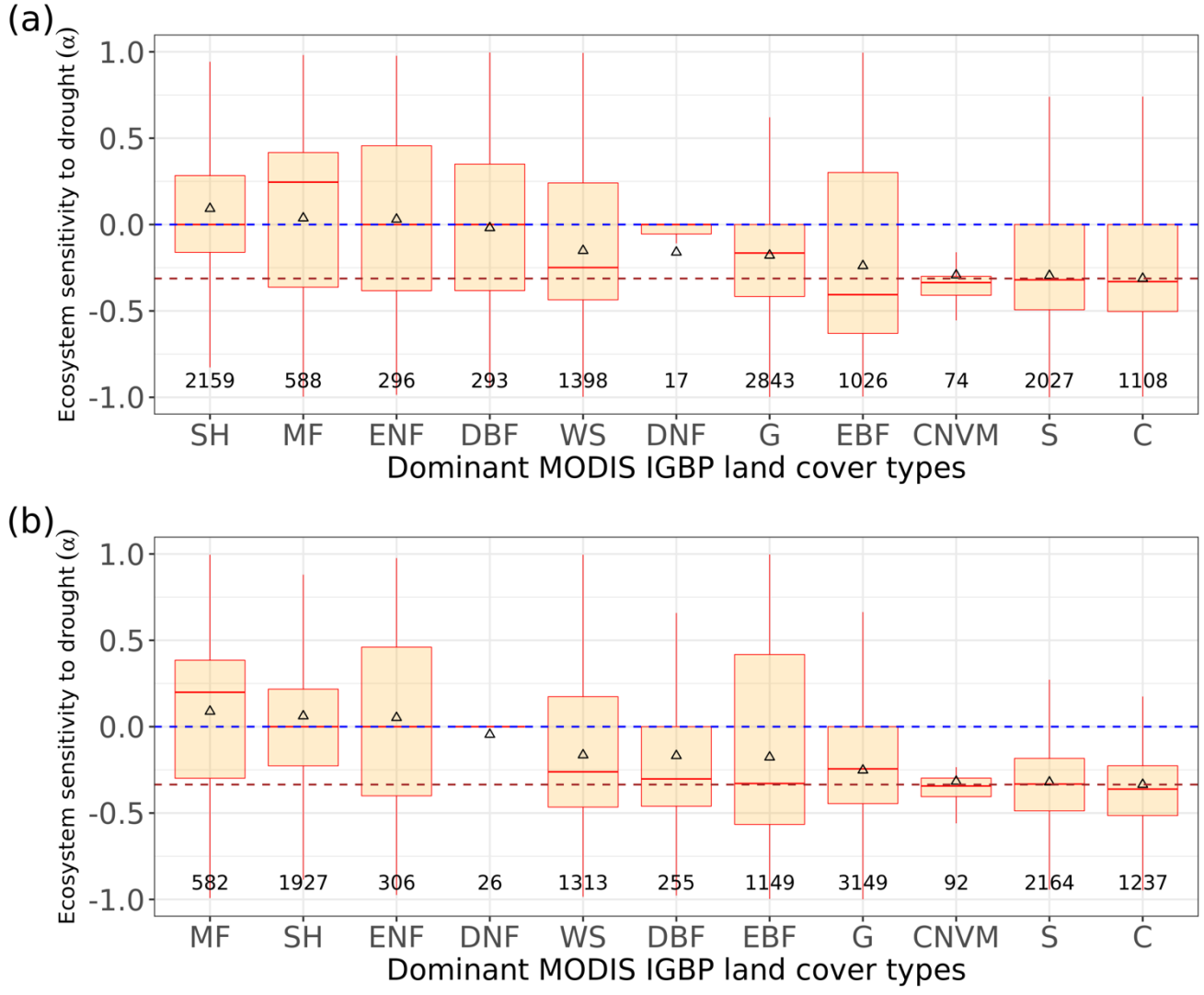

485 **Figure A3.** Distribution of ecosystem resistance α from (a) EVI and (b) kNDVI to drought for different dominant IGBP vegetation classes. Only significant α from the linear AR1 model is selected (P value<0.05) are shown.

https://doi.org/10.5194/egusphere-2023-304
Preprint. Discussion started: 28 March 2023

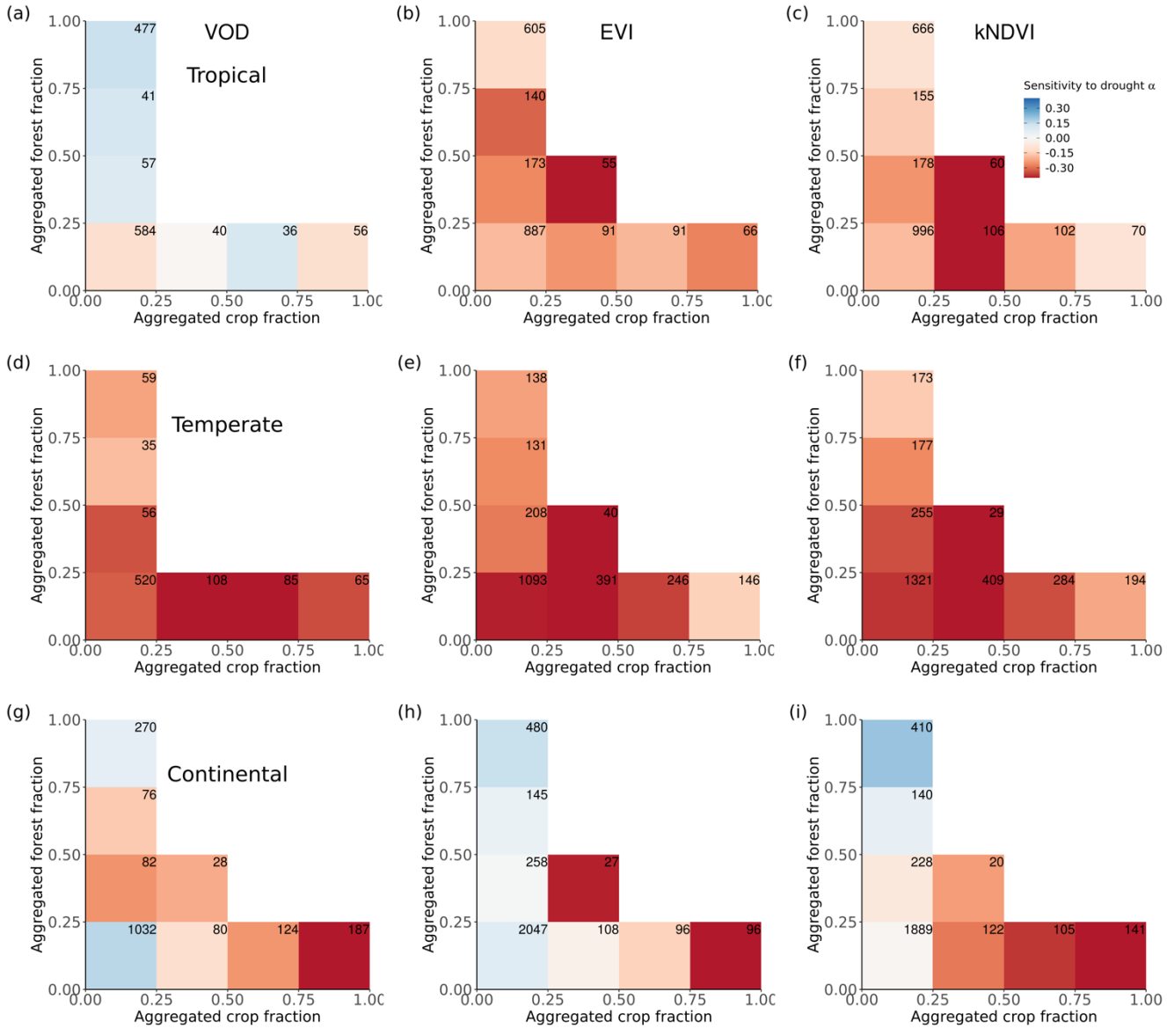

Figure A4. Ecosystem resistance to drought binned for different levels of the aggregated forest and cropland fraction classes from the three land cover products (a) L-VOD, (b) EVI and (c) kNDVI for Koeppen main climate class tropical climate and (d-f) for the temperate climate and (g-i) for the continental climate. Only significant coefficients α in the linear AR1 model (P value<0.05) are included and groups with less than 20 pixels are excluded.

https://doi.org/10.5194/egusphere-2023-304
Preprint. Discussion started: 28 March 2023

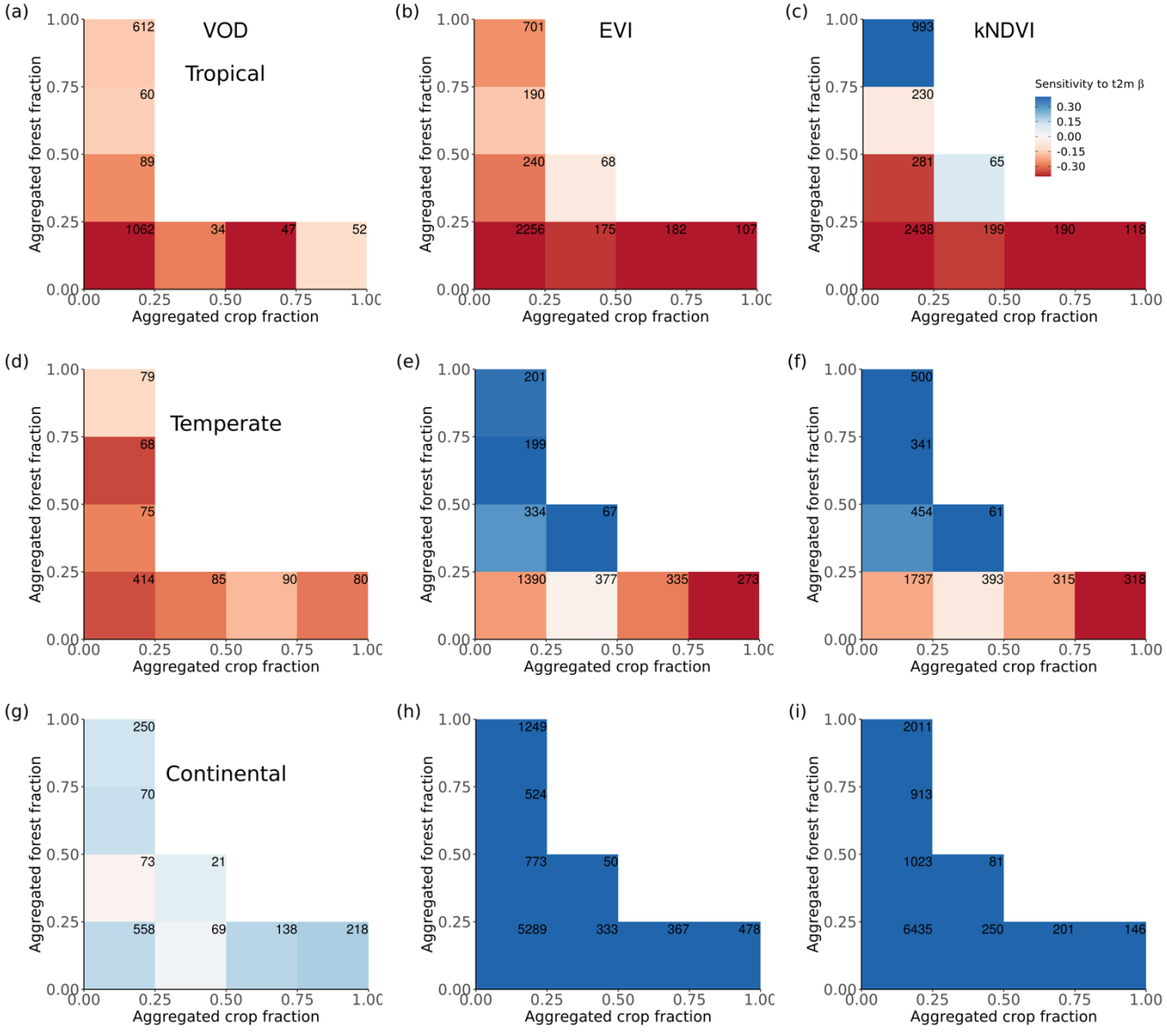

Figure A5. Ecosystem resistance to 2 m air temperature binned for different levels of the aggregated forest and cropland fraction classes from the three land cover products (a) L-VOD, (b) EVI and (c) kNDVI for Koeppen main climate class tropical climate and (d-f) for the temperate climate and (g-i) for the continental climate. Only significant coefficients β in the linear AR1 model (P value<0.05) are included and groups with less than 20 pixels are excluded.

https://doi.org/10.5194/egusphere-2023-304
Preprint. Discussion started: 28 March 2023

Code and data availability. The reconstructed SMOS L-VOD data are available upon request from Dr. Yang (huiyang@bgc-jena.mpg.de). MODIS EVI and NDVI data are freely available from https://modis.gsfc.nasa.gov/data/dataprod/mod13.php. ERA5 reanalysis data are freely available from https://www.ecmwf.int/en/forecasts/datasets/reanalysis-datasets/era5. MCD12Q1 land cover product is freely available from https://lpdaac.usgs.gov/products/mcd12q1v006/. ESA Land Cover CCI product is freely available from https://www.esa-landcover-cci.org/?q=node/164. LUH2 v2h land cover product is freely available from https://luh.umd.edu/data.shtml. The definitions of the AR6 reference sub-regions regions, the code and the spatially aggregated datasets are available at the GitHub ATLAS repository: https://github.com/SantanderMetGroup/ATLAS, https://doi.org/10.5281/zenodo.3998463 (Iturbide et al., 2020) under the Creative Commons Attribution (CC-BY) 4.0 licence. The global map of irrigation areas is freely available from https://www.fao.org/aquastat/ru/geospatial-information/global-maps-irrigated-areas/latest-version/. The global forest age map is freely available from https://www.bgc-jena.mpg.de/geodb/projects/Home.php. The code used in this study is available upon request.

Author contributions. CX, AB, SZ designed the study. CX implemented the method and performed the data analyses. HY, JPW provided the L-VOD data. HY processed and reconstructed the L-VOD data. CX, AB, SZ prepared the first draft, and all authors commented on the paper and provided feedback throughout the data analysis.

Competing interests. The authors declare that they have no conflict of interest.

Acknowledgements. Chenwei Xiao acknowledges support from the International Max Planck Research School for Global Biogeochemical Cycles. We would like to thank Christiane Schmullius for helpful and stimulating discussions. We thank Nuno Carvalhais for initial discussions about the use of vegetation proxies. We thank Ulrich Weber for the preparation of ERA5 data, MODIS land cover, NDVI and EVI data.

https://doi.org/10.5194/egusphere-2023-304
Preprint. Discussion started: 28 March 2023

References

Ahlström, A., Raupach, M. R., Schurgers, G., Smith, B., Arneth, A., Jung, M., Reichstein, M., Canadell, J. G., Friedlingstein, P., Jain, A. K., Kato, E., Poulter, B., Sitch, S., Stocker, B. D., Viovy, N., Wang, Y. P., Wiltshire, A., Zaehle, S., and Zeng, N.: The dominant role of semi-arid ecosystems in the trend and variability of the land CO2 sink, Science, 348, 895–899, https://doi.org/10.1126/science.aaa1668, 2015.

Allen, C. D., Macalady, A. K., Chenchouni, H., Bachelet, D., McDowell, N., Vennetier, M., Kitzberger, T., Rigling, A., Breshears, D. D., Hogg, E. H. (Ted), Gonzalez, P., Fensham, R., Zhang, Z., Castro, J., Demidova, N., Lim, J.-H., Allard, G., Running, S. W., Semerci, A., and Cobb, N.: A global overview of drought and heat-induced tree mortality reveals emerging climate change risks for forests, For. Ecol. Manag., 259, 660–684, https://doi.org/10.1016/j.foreco.2009.09.001, 2010.

Bastos, A., Fu, Z., Ciais, P., Friedlingstein, P., Sitch, S., Pongratz, J., Weber, U., Reichstein, M., Anthoni, P., Arneth, A., Haverd, V., Jain, A., Joetzjer, E., Knauer, J., Lienert, S., Loughran, T., McGuire, P. C., Obermeier, W., Padrón, R. S., Shi, H., Tian, H., Viovy, N., and Zaehle, S.: Impacts of extreme summers on European ecosystems: a comparative analysis of 2003, 2010 and 2018, Philos. Trans. R. Soc. B Biol. Sci., 375, 20190507, https://doi.org/10.1098/rstb.2019.0507, 2020.

Besnard, S., Koirala, S., Santoro, M., Weber, U., Nelson, J., Gütter, J., Herault, B., Kassi, J., N'Guessan, A., Neigh, C., Poulter, B., Zhang, T., and Carvalhais, N.: Mapping global forest age from forest inventories, biomass and climate data, Earth Syst. Sci. Data, 13, 4881–4896, https://doi.org/10.5194/essd-13-4881-2021, 2021.

Boisvenue, C. and Running, S. W.: Impacts of climate change on natural forest productivity – evidence since the middle of the 20th century, Glob. Change Biol., 12, 862–882, https://doi.org/10.1111/j.1365-2486.2006.01134.x, 2006.

Brandt, M., Wigneron, J.-P., Chave, J., Tagesson, T., Penuelas, J., Ciais, P., Rasmussen, K., Tian, F., Mbow, C., Al-Yaari, A., Rodriguez-Fernandez, N., Schurgers, G., Zhang, W., Chang, J., Kerr, Y., Verger, A., Tucker, C., Mialon, A., Rasmussen, L. V., Fan, L., and Fensholt, R.: Satellite passive microwaves reveal recent climate-induced carbon losses in African drylands, Nat. Ecol. Evol., 2, 827–835, https://doi.org/10.1038/s41559-018-0530-6, 2018.

Buermann, W., Forkel, M., O'Sullivan, M., Sitch, S., Friedlingstein, P., Haverd, V., Jain, A. K., Kato, E., Kautz, M., Lienert, S., Lombardozzi, D., Nabel, J. E. M. S., Tian, H., Wiltshire, A. J., Zhu, D., Smith, W. K., and Richardson, A. D.: Widespread seasonal compensation effects of spring warming on northern plant productivity, Nature, 562, 110–114, https://doi.org/10.1038/s41586-018-0555-7, 2018.

Camps-Valls, G., Campos-Taberner, M., Moreno-Martínez, Á., Walther, S., Duveiller, G., Cescatti, A., Mahecha, M. D., Muñoz-Marí, J., García-Haro, F. J., Guanter, L., Jung, M., Gamon, J. A., Reichstein, M., and Running, S. W.: A unified vegetation index for quantifying the terrestrial biosphere, Sci. Adv., 7, eabc7447, https://doi.org/10.1126/sciadv.abc7447, 2021.

Canadell, J., Jackson, R. B., Ehleringer, J. B., Mooney, H. A., Sala, O. E., and Schulze, E.-D.: Maximum rooting depth of vegetation types at the global scale, Oecologia, 108, 583–595, https://doi.org/10.1007/BF00329030, 1996.

Cheng, Y., Liu, L., Cheng, L., Fa, K., Liu, X., Huo, Z., and Huang, G.: A shift in the dominant role of atmospheric vapor pressure deficit and soil moisture on vegetation greening in China, J. Hydrol., 615, 128680, https://doi.org/10.1016/j.jhydrol.2022.128680, 2022.

Condit, R., Hubbell, S., and Foster, R.: Mortality-Rates of 205 Neotropical Tree and Shrub Species and the Impact of a Severe Drought, Ecol. Monogr., 65, 419–439, https://doi.org/10.2307/2963497, 1995.

https://doi.org/10.5194/egusphere-2023-304
Preprint. Discussion started: 28 March 2023

Denissen, J. M. C., Teuling, A. J., Pitman, A. J., Koirala, S., Migliavacca, M., Li, W., Reichstein, M., Winkler, A. J., Zhan, C., and Orth, R.: Widespread shift from ecosystem energy to water limitation with climate change, Nat. Clim. Change, 12, 677–684, https://doi.org/10.1038/s41558-022-01403-8, 2022.

DeSoto, L., Cailleret, M., Sterck, F., Jansen, S., Kramer, K., Robert, E. M. R., Aakala, T., Amoroso, M. M., Bigler, C., Camarero, J. J., Čufar, K., Gea-Izquierdo, G., Gillner, S., Haavik, L. J., Hereş, A.-M., Kane, J. M., Kharuk, V. I., Kitzberger, T., Klein, T., Levanič, T., Linares, J. C., Mäkinen, H., Oberhuber, W., Papadopoulos, A., Rohner, B., Sangüesa-Barreda, G., Stojanovic, D. B., Suárez, M. L., Villalba, R., and Martínez-Vilalta, J.: Low growth resilience to drought is related to future mortality risk in trees, Nat. Commun., 11, 545, https://doi.org/10.1038/s41467-020-14300-5, 2020.

Di Gregorio, A. and Jansen, L. J. M.: Land Cover Classification System (LCCS): Classification Concepts and User Manual, Food Agric. Org, 2005.

Didan, K.: MOD13C2 MODIS/Terra Vegetation Indices Monthly L3 Global 0.05P∘ CMG, NASA LP DAAC [data set], https://doi.org/10.5067/MODIS/MOD13C2.006, 2015 (https://ladsweb.modaps.eosdis.nasa.gov).

ESA: Land Cover CCI Product User Guide Version 2.0, available at: https://maps.elie.ucl.ac.be/CCI/viewer/download/ESACCI-LC-Ph2-PUGv2_2.0.pdf, last access: 19 December 2022.

Fan, L., Wigneron, J.-P., Ciais, P., Chave, J., Brandt, M., Fensholt, R., Saatchi, S. S., Bastos, A., Al-Yaari, A., Hufkens, K., Qin, Y., Xiao, X., Chen, C., Myneni, R. B., Fernandez-Moran, R., Mialon, A., Rodriguez-Fernandez, N. J., Kerr, Y., Tian, F., and Peñuelas, J.: Satellite-observed pantropical carbon dynamics, Nat. Plants, 5, 944–951, https://doi.org/10.1038/s41477-019-0478-9, 2019.

Flach, M., Sippel, S., Gans, F., Bastos, A., Brenning, A., Reichstein, M., and Mahecha, M. D.: Contrasting biosphere responses to hydrometeorological extremes: revisiting the 2010 western Russian heatwave, Biogeosciences, 15, 6067–6085, https://doi.org/10.5194/bg-15-6067-2018, 2018.

Forkel, M., Carvalhais, N., Rödenbeck, C., Keeling, R., Heimann, M., Thonicke, K., Zaehle, S., and Reichstein, M.: Enhanced seasonal CO2 exchange caused by amplified plant productivity in northern ecosystems, Science, 351, 696–699, https://doi.org/10.1126/science.aac4971, 2016.

Friedl, M., D. Sulla-Menashe. MCD12Q1 MODIS/Terra+Aqua Land Cover Type Yearly L3 Global 500m SIN Grid V006, NASA EOSDIS Land Processes DAAC [data set], https://doi.org/10.5067/MODIS/MCD12Q1.006. 2019.

Friedlingstein, P., O'Sullivan, M., Jones, M. W., Andrew, R. M., Gregor, L., Hauck, J., Le Quéré, C., Luijkx, I. T., Olsen, A., Peters, G. P., Peters, W., Pongratz, J., Schwingshackl, C., Sitch, S., Canadell, J. G., Ciais, P., Jackson, R. B., Alin, S. R., Alkama, R., Arneth, A., Arora, V. K., Bates, N. R., Becker, M., Bellouin, N., Bittig, H. C., Bopp, L., Chevallier, F., Chini, L. P., Cronin, M., Evans, W., Falk, S., Feely, R. A., Gasser, T., Gehlen, M., Gkritzalis, T., Gloege, L., Grassi, G., Gruber, N., Gürses, Ö., Harris, I., Hefner, M., Houghton, R. A., Hurtt, G. C., Iida, Y., Ilyina, T., Jain, A. K., Jersild, A., Kadono, K., Kato, E., Kennedy, D., Klein Goldewijk, K., Knauer, J., Korsbakken, J. I., Landschützer, P., Lefèvre, N., Lindsay, K., Liu, J., Liu, Z., Marland, G., Mayot, N., McGrath, M. J., Metzl, N., Monacci, N. M., Munro, D. R., Nakaoka, S.-I., Niwa, Y., O'Brien, K., Ono, T., Palmer, P. I., Pan, N., Pierrot, D., Pocock, K., Poulter, B., Resplandy, L., Robertson, E., Rödenbeck, C., Rodriguez, C., Rosan, T. M., Schwinger, J., Séférian, R., Shutler, J. D., Skjelvan, I., Steinhoff, T., Sun, Q., Sutton, A. J., Sweeney, C., Takao, S., Tanhua, T., Tans, P. P., Tian, X., Tian, H., Tilbrook, B., Tsujino, H., Tubiello, F., van der Werf, G. R., Walker, A. P., Wanninkhof, R., Whitehead, C., Willstrand Wranne, A., et al.: Global Carbon Budget 2022, Earth Syst. Sci. Data, 14, 4811–4900, https://doi.org/10.5194/essd-14-4811-2022, 2022.

https://doi.org/10.5194/egusphere-2023-304
Preprint. Discussion started: 28 March 2023

Gampe, D., Zscheischler, J., Reichstein, M., O'Sullivan, M., Smith, W. K., Sitch, S., and Buermann, W.: Increasing impact of warm droughts on northern ecosystem productivity over recent decades, Nat. Clim. Change, 11, 772–779, https://doi.org/10.1038/s41558-021-01112-8, 2021.

Gessler, A., Bottero, A., Marshall, J., and Arend, M.: The way back: recovery of trees from drought and its implication for acclimation, New Phytol., 228, 1704–1709, https://doi.org/10.1111/nph.16703, 2020.

Gibson, L., Lee, T. M., Koh, L. P., Brook, B. W., Gardner, T. A., Barlow, J., Peres, C. A., Bradshaw, C. J. A., Laurance, W. F., Lovejoy, T. E., and Sodhi, N. S.: Primary forests are irreplaceable for sustaining tropical biodiversity, Nature, 478, 378–381, https://doi.org/10.1038/nature10425, 2011.

Grossiord, C., Granier, A., Ratcliffe, S., Bouriaud, O., Bruelheide, H., Chećko, E., Forrester, D. I., Dawud, S. M., Finér, L., Pollastrini, M., Scherer-Lorenzen, M., Valladares, F., Bonal, D., and Gessler, A.: Tree diversity does not always improve resistance of forest ecosystems to drought, Proc. Natl. Acad. Sci., 111, 14812–14815, https://doi.org/10.1073/pnas.1411970111, 2014.

Hartley, A. J., MacBean, N., Georgievski, G., and Bontemps, S.: Uncertainty in plant functional type distributions and its impact on land surface models, Remote Sens. Environ., 203, 71–89, https://doi.org/10.1016/j.rse.2017.07.037, 2017.

Hersbach, H., Bell, B., Berrisford, P., Hirahara, S., Horányi, A., Muñoz-Sabater, J., Nicolas, J., Peubey, C., Radu, R., Schepers, D., Simmons, A., Soci, C., Abdalla, S., Abellan, X., Balsamo, G., Bechtold, P., Biavati, G., Bidlot, J., Bonavita, M., De Chiara, G., Dahlgren, P., Dee, D., Diamantakis, M., Dragani, R., Flemming, J., Forbes, R., Fuentes, M., Geer, A., Haimberger, L., Healy, S., Hogan, R. J., Hólm, E., Janisková, M., Keeley, S., Laloyaux, P., Lopez, P., Lupu, C., Radnoti, G., de Rosnay, P., Rozum, I., Vamborg, F., Villaume, S., and Thépaut, J.-N.: The ERA5 global reanalysis, Q. J. R. Meteorol. Soc., 146, 1999–2049, https://doi.org/10.1002/qj.3803, 2020.

Hurtt, G. C., Chini, L., Sahajpal, R., Frolking, S., Bodirsky, B. L., Calvin, K., Doelman, J. C., Fisk, J., Fujimori, S., Goldewijk, K. K., Hasegawa, T., Havlik, P., Heinimann, A., Humpenöder, F., Jungclaus, J., Kaplan, J., Kennedy, J., Kristzin, T., Lawrence, D., Lawrence, P., Ma, L., Mertz, O., Pongratz, J., Popp, A., Poulter, B., Riahi, K., Shevliakova, E., Stehfest, E., Thornton, P., Tubiello, F. N., van Vuuren, D. P., and Zhang, X.: Harmonization of Global Land-Use Change and Management for the Period 850–2100 (LUH2) for CMIP6, Climate and Earth System Modeling, https://doi.org/10.5194/gmd-2019-360, 2020.

Ingrisch, J. and Bahn, M.: Towards a Comparable Quantification of Resilience, Trends Ecol. Evol., 33, 251–259, https://doi.org/10.1016/j.tree.2018.01.013, 2018.

IPCC, 2021: Climate Change 2021: The Physical Science Basis. Contribution of Working Group I to the Sixth Assessment Report of the Intergovernmental Panel on Climate Change [Masson-Delmotte, V., P. Zhai, A. Pirani, S.L. Connors, C. Péan, S. Berger, N. Caud, Y. Chen, L. Goldfarb, M.I. Gomis, M. Huang, K. Leitzell, E. Lonnoy, J.B.R. Matthews, T.K. Maycock, T. Waterfield, O. Yelekçi, R. Yu, and B. Zhou (eds.)]. Cambridge University Press, Cambridge, United Kingdom and New York, NY, USA, 2391 pp. doi:10.1017/9781009157896, 2021.

Isbell, F., Craven, D., Connolly, J., Loreau, M., Schmid, B., Beierkuhnlein, C., Bezemer, T. M., Bonin, C., Bruelheide, H., de Luca, E., Ebeling, A., Griffin, J. N., Guo, Q., Hautier, Y., Hector, A., Jentsch, A., Kreyling, J., Lanta, V., Manning, P., Meyer, S. T., Mori, A. S., Naeem, S., Niklaus, P. A., Polley, H. W., Reich, P. B., Roscher, C., Seabloom, E. W., Smith, M. D., Thakur, M. P., Tilman, D., Tracy, B. F., van der Putten, W. H., van Ruijven, J., Weigelt, A., Weisser, W. W., Wilsey, B., and Eisenhauer, N.: Biodiversity increases the resistance of ecosystem productivity to climate extremes, Nature, 526, 574–577, https://doi.org/10.1038/nature15374, 2015.

https://doi.org/10.5194/egusphere-2023-304
Preprint. Discussion started: 28 March 2023

Iturbide, M., Gutiérrez, J. M., Alves, L. M., Bedia, J., Cerezo-Mota, R., Cimadevilla, E., Cofiño, A. S., Di Luca, A., Faria, S. H., Gorodetskaya, I. V., Hauser, M., Herrera, S., Hennessy, K., Hewitt, H. T., Jones, R. G., Krakovska, S., Manzanas, R., Martínez-Castro, D., Narisma, G. T., Nurhati, I. S., Pinto, I., Seneviratne, S. I., van den Hurk, B., and Vera, C. S.: An update of IPCC climate reference regions for subcontinental analysis of climate model data: definition and aggregated datasets, Earth Syst. Sci. Data, 12, 2959–2970, https://doi.org/10.5194/essd-12-2959-2020, 2020.

Jia, G., E. Shevliakova, P. Artaxo, N. De Noblet-Ducoudré, R. Houghton, J. House, K. Kitajima, C. Lennard, A. Popp, A. Sirin, R. Sukumar, L. Verchot: Land–climate interactions. In: Climate Change and Land: an IPCC special report on climate change, desertification, land degradation, sustainable land management, food security, and greenhouse gas fluxes in terrestrial ecosystems [P.R. Shukla, J. Skea, E. Calvo Buendia, V. Masson-Delmotte, H.-O. Pörtner, D.C. Roberts, P. Zhai, R. Slade, S. Connors, R. van Diemen, M. Ferrat, E. Haughey, S. Luz, S. Neogi, M. Pathak, J. Petzold, J. Portugal Pereira, P. Vyas, E. Huntley, K. Kissick, M, Belkacemi, J. Malley, (eds.)]. In press.In Press, pp. 131–248, www.ipcc.ch/srccl/chapter/chapter-2, 2019.

Keenan, T. F., Gray, J., Friedl, M. A., Toomey, M., Bohrer, G., Hollinger, D. Y., Munger, J. W., O'Keefe, J., Schmid, H. P., Wing, I. S., Yang, B., and Richardson, A. D.: Net carbon uptake has increased through warming-induced changes in temperate forest phenology, Nat. Clim. Change, 4, 598–604, https://doi.org/10.1038/nclimate2253, 2014.

Konings, A. G., Holtzman, N. M., Rao, K., Xu, L., and Saatchi, S. S.: Interannual Variations of Vegetation Optical Depth are Due to Both Water Stress and Biomass Changes, Geophys. Res. Lett., 48, e2021GL095267, https://doi.org/10.1029/2021GL095267, 2021.

Li, W., MacBean, N., Ciais, P., Defourny, P., Lamarche, C., Bontemps, S., Houghton, R. A., and Peng, S.: Gross and net land cover changes in the main plant functional types derived from the annual ESA CCI land cover maps (1992–2015), Earth Syst. Sci. Data, 10, 219–234, https://doi.org/10.5194/essd-10-219-2018, 2018.

Li, X., Wigneron, J.-P., Frappart, F., Fan, L., Ciais, P., Fensholt, R., Entekhabi, D., Brandt, M., Konings, A. G., Liu, X., Wang, M., Al-Yaari, A., and Moisy, C.: Global-scale assessment and inter-comparison of recently developed/reprocessed microwave satellite vegetation optical depth products, Remote Sens. Environ., 253, 112208, https://doi.org/10.1016/j.rse.2020.112208, 2021.

Liu, D., Wang, T., Peñuelas, J., and Piao, S.: Drought resistance enhanced by tree species diversity in global forests, Nat. Geosci., 15, 800–804, https://doi.org/10.1038/s41561-022-01026-w, 2022.

Liu, F., Liu, H., Xu, C., Shi, L., Zhu, X., Qi, Y., and He, W.: Old-growth forests show low canopy resilience to droughts at the southern edge of the taiga, Glob. Change Biol., 27, 2392–2402, https://doi.org/10.1111/gcb.15605, 2021a.

Liu, L., Chen, X., Ciais, P., Yuan, W., Maignan, F., Wu, J., Piao, S., Wang, Y.-P., Wigneron, J.-P., Fan, L., Gentine, P., Yang, X., Gong, F., Liu, H., Wang, C., Tang, X., Yang, H., Ye, Q., He, B., Shang, J., and Su, Y.: Tropical tall forests are more sensitive and vulnerable to drought than short forests, Glob. Change Biol., n/a, https://doi.org/10.1111/gcb.16017, 2021b.

Liu, Y. Y., van Dijk, A. I. J. M., de Jeu, R. A. M., Canadell, J. G., McCabe, M. F., Evans, J. P., and Wang, G.: Recent reversal in loss of global terrestrial biomass, Nat. Clim. Change, 5, 470–474, https://doi.org/10.1038/nclimate2581, 2015.

Liu, Z., Chen, L., Smith, N. G., Yuan, W., Chen, X., Zhou, G., Alam, S. A., Lin, K., Zhao, T., Zhou, P., Chu, C., Ma, H., and Liu, J.: Global divergent responses of primary productivity to water, energy, and CO2, Environ. Res. Lett., 14, 124044, https://doi.org/10.1088/1748-9326/ab57c5, 2019.

https://doi.org/10.5194/egusphere-2023-304
Preprint. Discussion started: 28 March 2023

Maherali, H., Pockman, W. T., and Jackson, R. B.: Adaptive Variation in the Vulnerability of Woody Plants to Xylem Cavitation, Ecology, 85, 2184–2199, https://doi.org/10.1890/02-0538, 2004.

McDowell, N., Pockman, W. T., Allen, C. D., Breshears, D. D., Cobb, N., Kolb, T., Plaut, J., Sperry, J., West, A., Williams, D. G., and Yepez, E. A.: Mechanisms of plant survival and mortality during drought: why do some plants survive while others succumb to drought?, New Phytol., 178, 719–739, https://doi.org/10.1111/j.1469-8137.2008.02436.x, 2008.

McDowell, N. G. and Allen, C. D.: Darcy's law predicts widespread forest mortality under climate warming, Nat. Clim. Change, 5, 669–672, https://doi.org/10.1038/nclimate2641, 2015.

Mueller, N. D., Butler, E. E., McKinnon, K. A., Rhines, A., Tingley, M., Holbrook, N. M., and Huybers, P.: Cooling of US Midwest summer temperature extremes from cropland intensification, Nat. Clim. Change, 6, 317–322, https://doi.org/10.1038/nclimate2825, 2016.

Nepstad, D. C., Tohver, I. M., Ray, D., Moutinho, P., and Cardinot, G.: Mortality of Large Trees and Lianas Following Experimental Drought in an Amazon Forest, Ecology, 88, 2259–2269, https://doi.org/10.1890/06-1046.1, 2007.

Nunes, M. H., Camargo, J. L. C., Vincent, G., Calders, K., Oliveira, R. S., Huete, A., Mendes de Moura, Y., Nelson, B., Smith, M. N., Stark, S. C., and Maeda, E. E.: Forest fragmentation impacts the seasonality of Amazonian evergreen canopies, Nat. Commun., 13, 917, https://doi.org/10.1038/s41467-022-28490-7, 2022.

Phillips, O. L., Aragão, L. E. O. C., Lewis, S. L., Fisher, J. B., Lloyd, J., López-González, G., Malhi, Y., Monteagudo, A., Peacock, J., Quesada, C. A., van der Heijden, G., Almeida, S., Amaral, I., Arroyo, L., Aymard, G., Baker, T. R., Bánki, O., Blanc, L., Bonal, D., Brando, P., Chave, J., de Oliveira, Á. C. A., Cardozo, N. D., Czimczik, C. I., Feldpausch, T. R., Freitas, M. A., Gloor, E., Higuchi, N., Jiménez, E., Lloyd, G., Meir, P., Mendoza, C., Morel, A., Neill, D. A., Nepstad, D., Patiño, S., Peñuela, M. C., Prieto, A., Ramírez, F., Schwarz, M., Silva, J., Silveira, M., Thomas, A. S., Steege, H. ter, Stropp, J., Vásquez, R., Zelazowski, P., Dávila, E. A., Andelman, S., Andrade, A., Chao, K.-J., Erwin, T., Di Fiore, A., C., E. H., Keeling, H., Killeen, T. J., Laurance, W. F., Cruz, A. P., Pitman, N. C. A., Vargas, P. N., Ramírez-Angulo, H., Rudas, A., Salamão, R., Silva, N., Terborgh, J., and Torres-Lezama, A.: Drought Sensitivity of the Amazon Rainforest, Science, 323, 1344–1347, https://doi.org/10.1126/science.1164033, 2009.

Piao, S., Fang, J., and He, J.: Variations in Vegetation Net Primary Production in the Qinghai-Xizang Plateau, China, from 1982 to 1999, Clim. Change, 74, 253–267, https://doi.org/10.1007/s10584-005-6339-8, 2006.

Piao, S., Liu, Z., Wang, T., Peng, S., Ciais, P., Huang, M., Ahlstrom, A., Burkhart, J. F., Chevallier, F., Janssens, I. A., Jeong, S.-J., Lin, X., Mao, J., Miller, J., Mohammat, A., Myneni, R. B., Peñuelas, J., Shi, X., Stohl, A., Yao, Y., Zhu, Z., and Tans, P. P.: Weakening temperature control on the interannual variations of spring carbon uptake across northern lands, Nat. Clim. Change, 7, 359–363, https://doi.org/10.1038/nclimate3277, 2017.

Poulter, B., Frank, D., Ciais, P., Myneni, R. B., Andela, N., Bi, J., Broquet, G., Canadell, J. G., Chevallier, F., Liu, Y. Y., Running, S. W., Sitch, S., and van der Werf, G. R.: Contribution of semi-arid ecosystems to interannual variability of the global carbon cycle, Nature, 509, 600–603, https://doi.org/10.1038/nature13376, 2014.

Poulter, B., MacBean, N., Hartley, A., Khlystova, I., Arino, O., Betts, R., Bontemps, S., Boettcher, M., Brockmann, C., Defourny, P., Hagemann, S., Herold, M., Kirches, G., Lamarche, C., Lederer, D., Ottlé, C., Peters, M., and Peylin, P.: Plant functional type classification for earth system models: results from the European Space Agency's Land Cover Climate Change Initiative, Geosci. Model Dev., 8, 2315–2328, https://doi.org/10.5194/gmd-8-2315-2015, 2015.

https://doi.org/10.5194/egusphere-2023-304
Preprint. Discussion started: 28 March 2023

Qin, Y., Xiao, X., Wigneron, J.-P., Ciais, P., Brandt, M., Fan, L., Li, X., Crowell, S., Wu, X., Doughty, R., Zhang, Y., Liu, F., Sitch, S., and Moore, B.: Carbon loss from forest degradation exceeds that from deforestation in the Brazilian Amazon, Nat. Clim. Change, 11, 442–448, https://doi.org/10.1038/s41558-021-01026-5, 2021.

Reichstein, M., Bahn, M., Ciais, P., Frank, D., Mahecha, M. D., Seneviratne, S. I., Zscheischler, J., Beer, C., Buchmann, N., Frank, D. C., Papale, D., Rammig, A., Smith, P., Thonicke, K., van der Velde, M., Vicca, S., Walz, A., and Wattenbach, M.: Climate extremes and the carbon cycle, Nature, 500, 287–295, https://doi.org/10.1038/nature12350, 2013.

Rodríguez-Fernández, N. J., Mialon, A., Mermoz, S., Bouvet, A., Richaume, P., Al Bitar, A., Al-Yaari, A., Brandt, M., Kaminski, T., Le Toan, T., Kerr, Y. H., and Wigneron, J.-P.: An evaluation of SMOS L-band vegetation optical depth (L-VOD) data sets: high sensitivity of L-VOD to above-ground biomass in Africa, Biogeosciences, 15, 4627–4645, https://doi.org/10.5194/bg-15-4627-2018, 2018.

Schwalm, C. R., Williams, C. A., Schaefer, K., Baldocchi, D., Black, T. A., Goldstein, A. H., Law, B. E., Oechel, W. C., Paw U, K. T., and Scott, R. L.: Reduction in carbon uptake during turn of the century drought in western North America, Nat. Geosci., 5, 551–556, https://doi.org/10.1038/ngeo1529, 2012.

Sherwood, S. C., Dixit, V., and Salomez, C.: The global warming potential of near-surface emitted water vapour, Environ. Res. Lett., 13, 104006, https://doi.org/10.1088/1748-9326/aae018, 2018.

Shukla, P.R., J. Skea, R. Slade, R. van Diemen, E. Haughey, J. Malley, M. Pathak, J. Portugal Pereira (eds.) Technical Summary, 2019. In: Climate Change and Land: an IPCC special report on climate change, desertification, land degradation, sustainable land management, food security, and greenhouse gas fluxes in terrestrial ecosystems [P.R. Shukla, J. Skea, E. Calvo Buendia, V. Masson-Delmotte, H.-O. Pörtner, D. C. Roberts, P. Zhai, R. Slade, S. Connors, R. van Diemen, M. Ferrat, E. Haughey, S. Luz, S. Neogi, M. Pathak, J. Petzold, J. Portugal Pereira, P. Vyas, E. Huntley, K. Kissick, M, Belkacemi, J. Malley, (eds.)]. In press, 2019.

Siebert, S., Henrich, V., Frenken, K., and Burke, J.: Update of the digital global map of irrigation areas to version 5., https://doi.org/10.13140/2.1.2660.6728, 2013.

Slette, I. J., Post, A. K., Awad, M., Even, T., Punzalan, A., Williams, S., Smith, M. D., and Knapp, A. K.: How ecologists define drought, and why we should do better, Glob. Change Biol., 25, 3193–3200, https://doi.org/10.1111/gcb.14747, 2019.

Teuling, A. J., Seneviratne, S. I., Stöckli, R., Reichstein, M., Moors, E., Ciais, P., Luyssaert, S., van den Hurk, B., Ammann, C., Bernhofer, C., Dellwik, E., Gianelle, D., Gielen, B., Grünwald, T., Klumpp, K., Montagnani, L., Moureaux, C., Sottocornola, M., and Wohlfahrt, G.: Contrasting response of European forest and grassland energy exchange to heatwaves, Nat. Geosci., 3, 722–727, https://doi.org/10.1038/ngeo950, 2010.

Thoning, K. W., Tans, P. P., and Komhyr, W. D.: Atmospheric carbon dioxide at Mauna Loa Observatory: 2. Analysis of the NOAA GMCC data, 1974–1985, J. Geophys. Res. Atmospheres, 94, 8549–8565, https://doi.org/10.1029/JD094iD06p08549, 1989.

Tian, F., Brandt, M., Liu, Y. Y., Rasmussen, K., and Fensholt, R.: Mapping gains and losses in woody vegetation across global tropical drylands, Glob. Change Biol., 23, 1748–1760, https://doi.org/10.1111/gcb.13464, 2017.

Tian, F., Wigneron, J.-P., Ciais, P., Chave, J., Ogée, J., Peñuelas, J., Ræbild, A., Domec, J.-C., Tong, X., Brandt, M., Mialon, A., Rodriguez-Fernandez, N., Tagesson, T., Al-Yaari, A., Kerr, Y., Chen, C., Myneni, R. B., Zhang, W., Ardö, J., and Fensholt, R.: Coupling of ecosystem-scale plant water storage and leaf phenology observed by satellite, Nat. Ecol. Evol., 2, 1428–1435, https://doi.org/10.1038/s41559-018-0630-3, 2018.

https://doi.org/10.5194/egusphere-2023-304
Preprint. Discussion started: 28 March 2023

Walther, S., Duveiller, G., Jung, M., Guanter, L., Cescatti, A., and Camps-Valls, G.: Satellite Observations of the Contrasting Response of Trees and Grasses to Variations in Water Availability, Geophys. Res. Lett., 46, 1429–1440, https://doi.org/10.1029/2018GL080535, 2019.

765 Wigneron, J.-P., Fan, L., Ciais, P., Bastos, A., Brandt, M., Chave, J., Saatchi, S., Baccini, A., and Fensholt, R.: Tropical forests did not recover from the strong 2015–2016 El Niño event, Sci. Adv., 6, eaay4603, https://doi.org/10.1126/sciadv.aay4603, 2020.

Wigneron, J.-P., Li, X., Frappart, F., Fan, L., Al-Yaari, A., De Lannoy, G., Liu, X., Wang, M., Le Masson, E., and Moisy, C.: SMOS-IC data record of soil moisture and L-VOD: Historical development, applications and perspectives, Remote
770 Sens. Environ., 254, 112238, https://doi.org/10.1016/j.rse.2020.112238, 2021.

Xu, L., Saatchi, S. S., Yang, Y., Yu, Y., Pongratz, J., Bloom, A. A., Bowman, K., Worden, J., Liu, J., Yin, Y., Domke, G., McRoberts, R. E., Woodall, C., Nabuurs, G.-J., de-Miguel, S., Keller, M., Harris, N., Maxwell, S., and Schimel, D.: Changes in global terrestrial live biomass over the 21st century, Sci. Adv., 7, eabe9829, https://doi.org/10.1126/sciadv.abe9829, 2021.

775 Zamora-Pereira, J. C., Yousefpour, R., Cailleret, M., Bugmann, H., and Hanewinkel, M.: Magnitude and timing of density reduction are key for the resilience to severe drought in conifer-broadleaf mixed forests in Central Europe, Ann. For. Sci., 78, 68, https://doi.org/10.1007/s13595-021-01085-w, 2021.

Zeng, Y., Hao, D., Huete, A., Dechant, B., Berry, J., Chen, J. M., Joiner, J., Frankenberg, C., Bond-Lamberty, B., Ryu, Y., Xiao, J., Asrar, G. R., and Chen, M.: Optical vegetation indices for monitoring terrestrial ecosystems globally, Nat. Rev.
780 Earth Environ., 1–17, https://doi.org/10.1038/s43017-022-00298-5, 2022.

Zhang, F., Quan, Q., Ma, F., Tian, D., Hoover, D. L., Zhou, Q., and Niu, S.: When does extreme drought elicit extreme ecological responses?, J. Ecol., 107, 2553–2563, https://doi.org/10.1111/1365-2745.13226, 2019.

Zhang, Y., Xiao, X., Zhou, S., Ciais, P., McCarthy, H., and Luo, Y.: Canopy and physiological controls of GPP during drought and heat wave, Geophys. Res. Lett., 43, 3325–3333, https://doi.org/10.1002/2016GL068501, 2016.

785 Zhu, J., Zhang, M., Zhang, Y., Zeng, X., and Xiao, X.: Response of Tropical Terrestrial Gross Primary Production to the Super El Niño Event in 2015, J. Geophys. Res. Biogeosciences, 123, 3193–3203, https://doi.org/10.1029/2018JG004571, 2018.

Zscheischler, J., Reichstein, M., Harmeling, S., Rammig, A., Tomelleri, E., and Mahecha, M. D.: Extreme events in gross primary production: a characterization across continents, Biogeosciences, 11, 2909–2924, https://doi.org/10.5194/bg-11-
790 2909-2014, 2014.